Dissertation for the Doctoral Degree

Studies on Enhancement of Phagocytosis and Cytotoxicity in Macrophages by IL-18-Stimulation.

Name: Xu Henan

Doctoral Program in Life and Food Science

Graduate School of Science and Technology

Niigata University

Abbreviation

IL-18	Interleukin-18
Casp-1	Caspase-1
Tnf-α	Tumor necrosis factor
IL-6	Interleukin-6
Nos2	Inducible nitric oxide synthase
Arg-1	Arginase-1
IL-10	Interleukin-10
TAM	Tumor-associated macrophages
CM	Conditioned medium
H.E.	Hematoxylin and Eosin
FACS analysis	Flow cytometry analysis
1400w	N-(3-[Aminomethyl]benzyl)acetamidine (Nos2 inhibitor)

Abstract

Inoculation of mice with the murine NFSA cell line caused the formation of large tumors with necrotic tumor cores. FACS analysis revealed accumulations of $CD11b^+$ cells in the tumors. Microarray analysis indicated that the NFSA cells expressed a high level of the pro-inflammatory factor *interleukin-18* (*il-18*), which is known to play a critical role in macrophages. However, little is known about the physiological function of IL-18-stimulated macrophages. Here, we provide direct evidence that IL-18 enhances the phagocytosis of RAW264 cells and peritoneal macrophages, accompanied by the increased expression of *tumor necrosis factor* (*tnf-α*), *interleukin-6* (*il-6*) and *inducible nitric oxide synthase* (*Nos2*). IL-18-stimulated RAW264 cells showed an enhanced cytotoxicity to endothelial F-2 cells via direct cell-to-cell interaction and the secretion of soluble mediators, including NOS2 derived NO. Taken together, these results demonstrate that tumor-derived IL-18 plays an important role in the phagocytosis of macrophages and that IL-18-stimulated macrophages may damage tumor endothelial cells.

概要

マウス培養細胞株，NFSA 細胞をマウス皮下に移植すると巨大な腫瘍を形成し，その中心部は壊死を起こす。FACS（自動細胞解析捕集装置）を用いてこのNFSA腫瘍中の細胞を解析すると，マクロファージなどに発現の認められる CD11b 陽性細胞の蓄積があることが判った。NFSA 細胞で発現している遺伝子を DNA マイクロアレイ解析により解析すると，マクロファージで重要な役割を担うことが知られている炎症性インターロイキン-18（IL-18）を高発現していた。以上の結果から，IL-18 とマクロファージの関係が予想されたが，これまでに IL-18 により活性化されたマクロファージがどのような生理活性を担うかについては詳細に解明されていない。

本論文ではIL-18がマクロファージ細胞株であるRAW264細胞およびFACSにより単離したマウス腹腔由来マクロファージの貪食作用を強化することを，これらの細胞への蛍光マイクロビーズの取り込みを測定することにより明らかにした。このとき，この IL-18 により活性化されたマクロファージでは腫瘍壊死因子（TNF-α），インターロイキン-6（IL-6）および誘導可能な一酸化窒素合成酵素（Nos2）等の遺伝子発現も増加することを明らかにするとともに，抗 IL-18 中和抗体を用いた実験から，これらが IL-18 の作用によるものであることを明確に示した。さらに，IL-18 で刺激された RAW264 細胞を血管内皮細胞株 F-2 と共培養すると，細胞間相互作用により F-2 細胞はマクロファージにより傷害される事を明らかにした。また，共培養時に RAW264 細胞と F-2 細胞の直接接触を妨げた場合も，RAW264 細胞は F-2 細胞に対する傷害性を示したことから，マクロファージにより産生される何らかの可溶性物質もこの傷害に関与しているものと考えられた。これらを総合すると，IL-18 刺激によりマクロファージの貪食能は増強されるとともに，血管内皮細胞に対して液性因子や細胞間相互作用を介して傷害を及ぼすことが明らかとなった。従って，高い IL-18 産生能を示す NFSA 腫瘍においては，この IL-18 により腫瘍中のマクロファージが活性化されその細胞障

害性活性が上昇して血管内皮細胞が傷害を受けることにより血管新生が阻害され，その結果，腫瘍細胞の壊死が誘導されると予想される。

1 Introduction

1.1 Role of Macrophages in Tumors

Tumor promotion relies on the formation of new blood vessels and lymphatic vessels for an adequate supply of oxygen and nutrients (1, 2). This process is tightly attuned by both the remodeling of pre-existed vasculatures and the recruitment of cells originating from bone marrow-derived cells (BMDCs) (3). Macrophages constitute a large portion of the infiltrated heterogeneous inflammatory cell populations in the tumor site and play an important part in both tumor initiation and various key steps in the growth and metastasis (4), termed as tumor-associated macrophages (TAM) (5). Following recruitment to the tumor, monocytes are educated by the tumor microenvironment and subsequently differentiated into distinct types of macrophages, which played unique physiological roles, such as protecting the host from infection and tumors by activating the immune response (that is M1-type macrophages) or, conversely, promoting tumor progression (that is M2-type macrophages) (**Fig. 1**) (6, 7, 8, 9). Although it is needed that the entire feature of TAM would be further elucidated, many experimental evidences suggested that tumor microenvironment switched the phenotype of TAM to the M2-type macrophages, which have strong tumor progression activity than the M1-type macrophages (10, 11).

The M1 or “Classically activated” macrophages are triggered by Interferon gamma (IFN-γ), microbial products, Lipopolysaccharides (LPS) (12) or TNF-α (13), and mediated by several signal transduction pathways, such as signal transducer and activated protein of transcription (STAT), nuclear factor kappa-light-chain-enhancer of activated B cells (NF-κB), and mitogen-activated protein kinases (MAPK) (13, 14, 15). The M1 macrophages are characterized the release of the inflammatory cytokines and tumoricidal activity (4). They have high capacity to present antigen,

involved in the responses of type I helper T (Th1) cells (16), high production of nitric oxide (NO), and the ability to kill pathogens and cells (17).

In contrast, the M2 or “Alternatively activated” TAM are induced by various stimuli, such as IL-4 together with IL-13 (18), immune complex or glucocorticoid (19). M2 macrophages are characterized as the macrophages which expressed high arginase (I and II) among other markers, which is accompanied with low expression of iNOS (20). The M2 macrophages have a immunosuppressive properties (21) by producing anti-inflammatory factors, facilitated malignancy by stimulating angiogenesis and suppressing antitumor immune response (22).

As it is a vital process in tumor growth, angiogenesis has been the target of many anti-tumor therapies in recent years. Over the past decade, macrophages have been recognized as critical regulators that break the balance between pro- and anti-angiogenesis through the secretion of multiple cytokines, matrix metalloproteinase (23), reactive oxygen species (ROS) and nitric oxide (NO) (8). The TAM are now considered as a hallmark target for cancer immunotherapy (24). The reduction of their tumor-promoting activities (that is M2-phenotype) and induction of their M1-like tumoricidal activity has become a hot study area (24, 25).

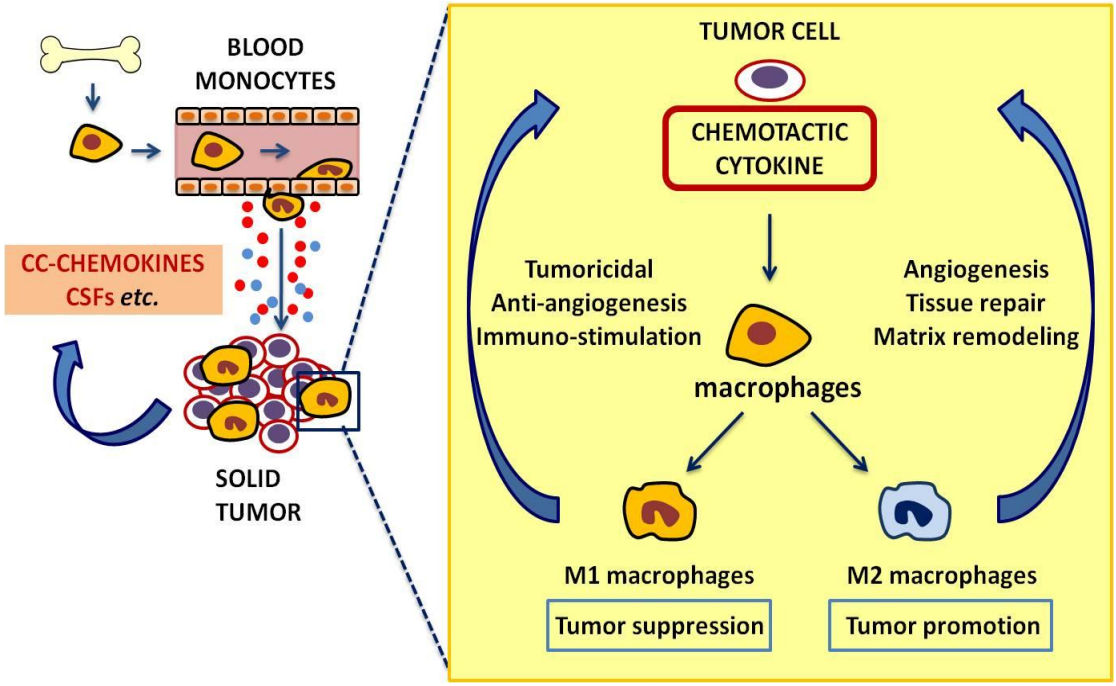

Figure 1. **The roles of macrophages in solid tumors.**
Tumor-derived chemokines and colony stimulating factors (CSFs), actively recruit circulating blood monocytes into the tumor. In the tumor site, monocytes were educated by the tumor microenvironment and subsequently differentiated into distinct type of macrophages, where they modulated tumor promotion and establish relationships with tumor cells. Figure was modified and adapted from Sica *et al* (9).

1.2 Functions of IL-18

The IL-18, a member of the IL-1 super family, is initially characterized as a potent inducer of IFN-γ, and is produced by T cells, activated macrophages, Kupffer cells (26, 27), dendritic cells (28), Natural killer (NK) cells (29) and damaged endothelial cells (30). As shown in **Figure 2**, IL-18 was firstly synthesized as a bio-inactive precursor that undergoes proteolytic cleavage by the intracellular protease caspase-1 (Casp-1) to generate a mature, biologically active cytokine (31, 32, 33). As an immunostimulatory cytokine, IL-18 contributes to the activation of macrophages to uptake pathogen and the release of nitrogen radicals and toxic oxygen (34). It plays remarkable

important roles in host defense against infection and initiating Th1 and Th17 adaptive immune response (35). Furthermore, IL-18 has significant anti-tumor activity in numerous pre-clinical models. It plays pivotal roles in connecting inflammatory immune responses with tumor progression. Previous studies have reported that local IL-18 in the tumor environment significantly potentiates anti-tumor immunity mediated by innate and adaptive immune mechanisms in murine orthotopic prostate carcinomas (36). The transfer of the *IL-18* gene into tumor cells, alone (37, 38, 39) or in combination with the *IL-12* gene (40, 41), resulted in the inhibition of tumor progression. In murine melanoma, IL-18 exerts potential anti-tumor activity via the inhibition of angiogenesis (37). The direct injection of IL-18 into established tumors also inhibited tumor growth, which was associated with an increase in intratumoral macrophages but not T cells or NK cells (36).

In addition, IL-18 induces the expression of intercellular adhesion molecule-1 (ICAM-1) in monocytes (42), and also induces both ICAM-1 and VCAM-1 in endothelial cells (43), thus favoring tissue infiltration of immune cells. Some studies have revealed that IL-18, alone or in combination with IL-12, stimulates macrophages to produce high levels of IL-6, TNF-α (41, 44), Cxcl10 (45) and Nos2 (46), which are typically recognized as markers of classical activated macrophages and are responsible for the important anti-tumor functions.

Although increasing evidence suggests that IL-18 plays a critical role in macrophages behavior, it is rare that studies focused on the functions of IL-18-stimulated macrophages, especially with respect to phagocytosis and their interaction with endothelial cells.

In this report, the effects of exogenous IL-18 on function of macrophages *in vitro* were investigated. Here, I provide that exogenous IL-18 promoted phagocytosis in macrophages and enhanced cytotoxicity to the endothelial cells.

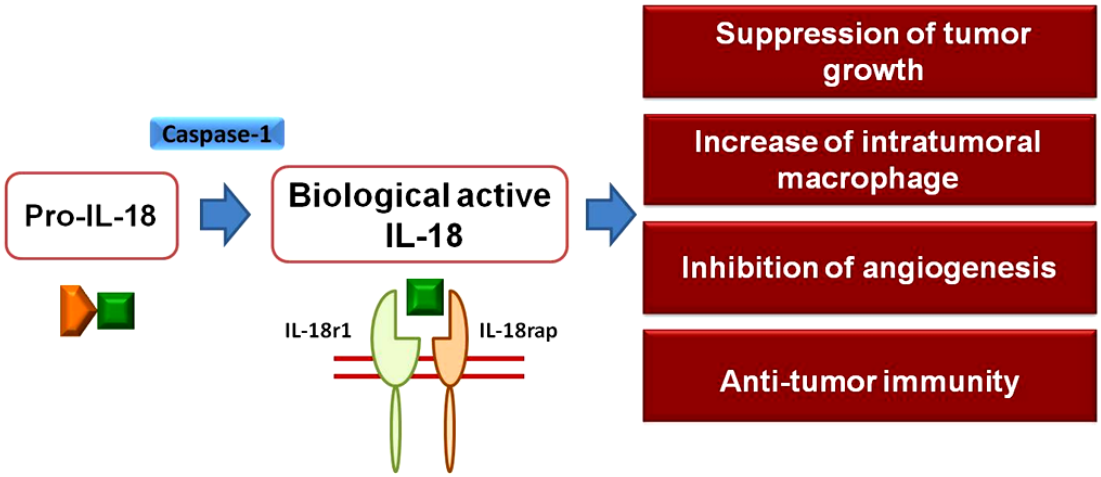

Figure 2. Production of biological active IL-18.

IL-18 is firstly synthesized as a 24-KD bio-inactive precursor. The intracellular protease caspase-1 (Casp-1) cleaves the signal peptides and generates biological active IL-18. The IL-18 receptor is heterodimer, and transduces the IL-18 signal.

2 Materials and Methods

2.1 Mice

The C3H/HeN strain mice were purchased from SLC (SLC Co. Ltd, Sizuoka, Japan) and bred in specific pathogen-free condition (SPF). Eight- to 12-week-old C3H/HeN mice were used in these experiments. The animal experiments were performed in compliance with the guidelines of Niigata University.

2.2 Cell lines

The murine monocyte/macrophage cell line RAW 264 (47) was obtained from the American Type Culture Collection (ATCC, Rockville, MD, USA) and maintained in Dulbecco's modified Eagle's medium (DMEM) (Gibco, CA, USA) supplemented with 10% (v/v) fetal bovine serum (FBS) and 2 mM L-glutamine. The murine fibrosarcoma cell line NFSA (48) was maintained in our laboratory and grown in alpha-modified Minimal essential medium (α-MEM) (Gibco, CA, USA) supplemented with 5% (v/v) FBS. The murine sarcoma cell line, MS-K, was established from a long-time culture of C3H/HeN mice bone marrow cells by our laboratory (49) grown in alpha-modified Minimal essential medium (α-MEM) supplemented with 5% (v/v) Horse serum (HS). The murine endothelial cell line F-2 (50) was cultured in RPMI-1640 (Gibco, CA, USA) supplemented with 5% FBS and used to create F-2-Orange cells. Briefly, F-2 cells were transfected with *pcDNA™6.2/V5* mammalian expression vector (Invitrogen, Tokyo, Japan), encoding the *Kusabira Orange* gene and G418 selection was done to select stable cell line (not published). Stable transformant expressed the fluorescent protein (Kusabira Orange). All the medium contained 100 U/mL penicillin and 100 µg/mL streptomycin (GIBCO). Cells were cultured at 37°C in humidified atmosphere in 5% (v/v) CO_2-incubator.

2.3 Preparation of peritoneal macrophages

The adherent cells were harvested from the peritoneal cavity of C3H/HeN with the pre-cold PBS. Then the cells were re-suspended in RPMI-1640 supplemented with 10%FBS, and, the cells were seeded into 60-mm dishes at a concentration of $1X10^7$ cells per dish for 2 hours at 37°C. After removing the non-adherent cells by washing, the adherent cells were detached from the dish with pre-cold EDTA/PBS and stained with biotin-conjugated-anti-mouse CD19 antibody (Miltenyi Biotec, USA) for 30 minutes at 4°C. Then the CD19-negative peritoneal adherent primary macrophages were separated by anti-biotin Microspheres (Miltenyi Biotec, USA) with MACS system following to the manufactory's instruction. The CD19-negative peritoneal macrophages were re-suspended in RPMI-1640 supplemented with 10% FBS and used for further analysis.

2.4 Tumorigenesis studies

NFSA and MS-K cells were harvested using 0.05% trypsin in EDTA/PBS, washed twice with PBS and re-suspended in cold-PBS. The number of cells and viability was determined by the trypan blue dye exclusion test. Subcutaneous inoculation of tumor cells was performed at both sides of the abdomen of each mouse in 100μL of cell suspension ($1X10^6$ cells/mouse/side). Each experimental group consisted of 7 mice. The tumor volume was calculated from the formula: Tumor Volume [mm^3] = (length [mm]) X (width [mm]) ^{2} X0.5. The mice were sacrificed at day 7, 9, 12 and 16 after inoculation.

2.5 Analysis of CD11b+ cells in tumors

The tumors were excised from the mice at day 7, 9, 12 and 16 after inoculation. Then the tumors were cut into pieces in cold-PBS mechanically. The cell suspension was treated with 120 unit/mL collagenase (Yakuruto,

Tokyo, Japan) for 30 minutes at 37°C. A single cell suspension was prepared and incubated with APC-conjugated-anti-mouse CD11b antibody (Beckman Coulter Inc. CA, USA) for 30 min at 4°C. Then the CD11b-positive (+) cells were analyzed and sorted by FACS Aria II (BD, Tokyo, Japan) for further analysis.

2.6 Histological analysis

Tumors generated by NFSA or MS-K cells were excised at day 12 post-inoculation and fixed in freshly prepared 4% paraformaldehyde in PBS at 4 °C for 24 hours. Then the tumors were dehydrated though a graded ethanol series (70%, 90%, 95%, 99% and 100%) and embedded in paraffin wax following standard procedures. Sections of 4-6 μm were stained with Hematoxylin and Eosin (H.E).

2.7 Preparation of conditioned medium (CM)

The MS-K or NFSA cells ($1X10^6$ cells/100mm dish) were cultured for 3 days with serum-containing medium. Then the supernatant was collected, and centrifuged at 2000 rpm at 4°C to remove the cell debris. Then the CM was stored at -30°C before use. In some experiments, heat-inactivated (56°C, 30 min) CM was prepared.

2.8 Interleukin-18 ELISA

The concentration of IL-18 in conditioned medium was determined by mouse IL-18 ELISA kit (MBL, Tokyo, Japan) following the manufacturer instructions.

2.9 Phagocytosis assay

RAW264 cells were plated at a density of $1X10^4$ cells per 35mm dish in DMEM supplemented with 10% FBS. After 24 hours of pre-incubation,

NFSA-CM, MS-K-CM or recombinant IL-18 (MBL, Tokyo, Japan) was added to the medium to stimulate the cells for 5 days. Meanwhile, the peritoneal macrophages were seeded at a density of $3X10^5$ cells per 35mm dish, and cultured for 5 days in RPMI-1640 supplemented with 10% FBS containing 20% CM or 10 ng/mL rIL-18. In some experiments, the neutralizing monoclonal anti-mouse IL-18 antibody (MBL, Tokyo, Japan) was added to the medium.

For analysis the phagocytosis in RAW264 cell line and primary macrophages *in vitro*, Fluoresbrite YG microspheres (2.5% solids [w/v]; Polysciences Inc., Tokyo, Japan) were used. Briefly, the microspheres were added to the medium at a final concentration of 100 beads per cell and incubated for 2 hours at 37°C in fresh medium. Then, the cells containing the microspheres were analyzed as FITC-positive cells by FACS Aria II (BD, Tokyo, Japan).

2.10 May-Grünwald-Giemsa staining

In some experiment, the microsphere-eating cells were resuspended with cold PBS supplemented 2% FBS, and the cyto-spin preparations were prepared and stained with May-Grünwald-Giemsa solution.

2.11 RNA extraction and preparation of cDNA

Total RNA from cell lines were isolated using TRIzol RNA Isolation Reagents (Invitrogen, USA). Total RNA from tumor derived CD11b-positive cells and CD19-negative peritoneal macrophages were isolated by ReliaPrep^{TM} RNA Cell Miniprep System (Promega, CA，USA) following the manufactures' instruction. DNase I-treated (TAKARA, Tokyo, Japan) RNA was transcribed to cDNA using a cDNA synthesis kit (TAKARA, Tokyo, Japan).

2.12 Analysis of gene expression by RT-PCR and quantitative PCR (qPCR)

The expression of *Nos2, IL-6, Cxcl10, tnf-α, IL-12p35, IL-12p40, IL-18r1, IL-18rap, Arg-1, IL-10 and beta-actin* was analyzed by RT-PCR with gene-specific PCR primers. Briefly, the reaction mixture contained 2XGoTaq® Green Master Mix (final 1X) (Promega, CA，USA), up-stream primers and down-stream primers (final 0.5μM, each), diluted cDNA template (1/10 volume diluted with distilled water) and distilled water. The amplification sequence was proper cycles of 94°C for 30-second, optimized annealing temperature for 30-second and 72°C for 30-second. The PCR product of samples was analyzed by electrophoresis in a 2% agarose gel and visualized by ethidium bromide staining.

In some experiments, the gene expression was quantitatively analyzed using a Light Cycler Real-Time PCR System (Roche Diagnostics GmbH, Germany). Briefly, cDNA was mixed with a gene-specific primer and SYBR Premix *Ex Taq* (TAKARA, Japan). Then, the relative expression of each gene compared to that of *beta-actin* was calculated. The primer sequences, annealing temperatures and product sizes are summarized in **Table 2**.

2.13 DNA chip analysis

DNA-free total RNA was prepared from MS-K or NFSA cells, and then labeled RNA probes were prepared for DNA chip analysis. The SurePrint G3 Mouse Gene Expression Microarray (Agilent, Tokyo, Japan) was used.

2.14 Direct co-culture of activated RAW264 cells with endothelial cells

F-2-Orange cells were cultured in 35-mm dishes for 24 hours at the proper density to obtain a monolayer of cells. Stimulated RAW264 cells were

prepared using rIL-18 (1 ng/mL) or 40% NFSA-CM and then overlaid onto the F-2-Orange cell monolayer at various ratio (RAW264:F-2-Orange = 0.1:1, 0.5:1 and 1:1). After 24 or 48 hours of incubation, the dishes were washed with PBS to remove the non-adherent cells, and the number of adherent F-2-Orange cells was analyzed by FACS.

2.15 Membrane-separated co-cultures of activated RAW264 cells with endothelial cells

The appropriate number of F-2-Orange cells was seeded in the lower chamber of a Transwell plate (0.4 μm pore size, Corning, NY, USA), and the plate was incubated for 24 hours to make a monolayer. Stimulated RAW264 cells, which were prepared as described above, were seeded in the upper chamber of the Transwell plate. After 48 hours of co-culture, the living F-2-Orange cells were counted using a hemocytometer. In some experiments, the 1400w was used to block the activity of NOS2 at a final concentration of 100μM as described before (51).

2.16 Statistical analysis

All of the data are expressed as the mean ± standard error of the mean (SEM). A student's *t* test was used to assess statistical significance for paired observations. Data for multiple comparisons were analyzed using ANOVA and Dunnett's post hoc test. In all comparisons, statistical significance was defined at $p<0.05$.

3 Results

3.1 *In vivo* tumorigenesis studies in mice

Tumors were generated by subcutaneously injection of MS-K or NFSA cells (1 x 10^6 cells/mouse/side) into both sides of the abdomen of each mouse. The tumors were excised from the mice at day 7, 9, 12 and 16. After inoculation, both the MS-K and NFSA cells formed the tumors with large volume under the flanks of C3H/HeN mice. As shown in figures, the MS-K tumor revealed abundant blood supply both around and inside the tumor. However, the NFSA tumor exhibited poor blood perfusion on day16 (**Fig. 3A, B**). Tumors were excised and embedded with paraffin, and then H.E-staining sections were prepared following the standard procedure. Histology analysis demonstrated that a well-developed blood vessel network was formed in the MS-K tumors, while necrosis occurred in the cores of the NFSA tumors (**Fig. 3A, B**). The tumor growth curve showed that MS-K tumor grew slowly in the early days after post-inoculation, and then it proliferated rapidly from day 12 to day 16. Contrary to this, the growth ratio of NFSA tumor was much more homogeneous (**Fig. 3C**).

3.2 Microarray analysis in tumor cell lines

To find out the responsible factors, the differential expression of genes in MS-K and NFSA cell lines was analyzed by SurePrint G3 microarray (**Table 1**). It revealed that MS-K and NFSA cells expressed almost the same level of *colony stimulating factor 1* (*Csf-1*/*M-csf*), which accompanied by a very low level expression of *colony stimulating factor 2* (*Csf-2*/*Gm-csf*) and *colony stimulating factor 3* (*G-csf*) (**Table 1.**). The colony stimulation factors, especially *Csf-1*, were well known as the major lineage regulator of macrophages (16, 52). However, NFSA cells highly expressed a series of chemokines than the MS-K cells (**Table 1.**). The major role of chemokines is

to act as chemoattractants for leukocytes, recruiting monocytes, neutrophils and other effector cells from the blood to tissue. In addition, compared with MS-K cells, NFSA cells produced a higher level of the pro-inflammatory factor, *interleukin-18* (*IL-18*) and *caspase-1* (*Casp-1*) (**Table 1.**), which was critical for the maturation of IL-18.

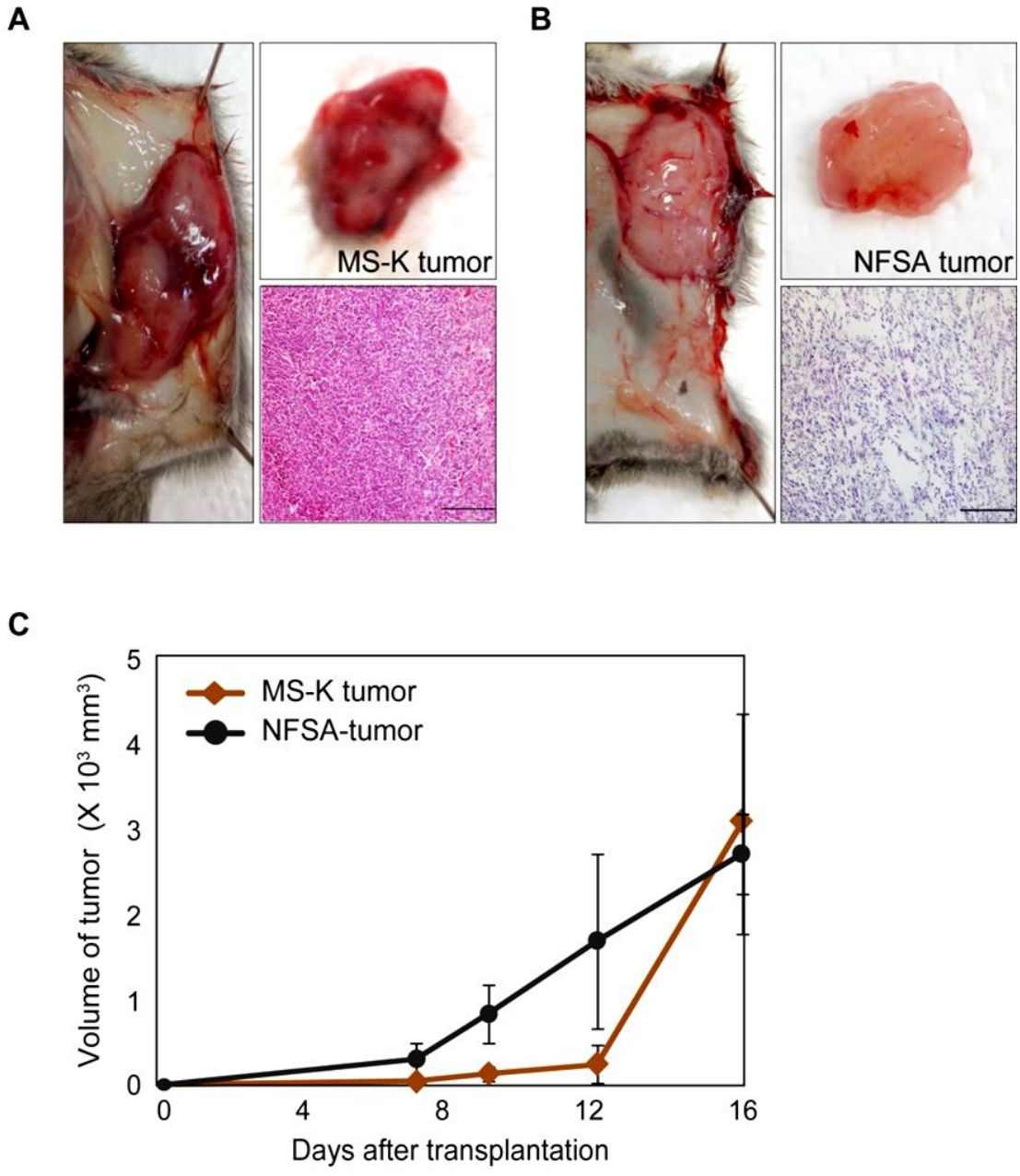

Figure 3. Tumorigenesis studies in C3H/HeN mice.

A. MS-K tumor on day16 (left). Histological analysis was performed by hematoxylin and eosin (H.E.) staining (lower right panel).

B. NFSA-tumor on day16 (left). Histological analysis was performed by H.E. stain (lower right panel).

C. Growth curves of tumors. Tumors were excised at 7, 9, 12 and 16 days after inoculation. All bars show the mean ± S.E. Asterisks denote significant differences, *: *p<0.05, **: p<0.005*.

3.3 Accumulation of CD11b+ cell population in tumors

The existence of the CD11b+ cells in NFSA or MS-K tumors was determined by FACS at day 9, day 12 and day 16. The results indicated that the accumulation of CD11b+ cells in the tumors was increased with tumor growth. More importantly, the number of CD11b+ cells was higher in the NFSA tumors than in the MS-K tumors during the whole tumor growth period (**Fig. 4**).

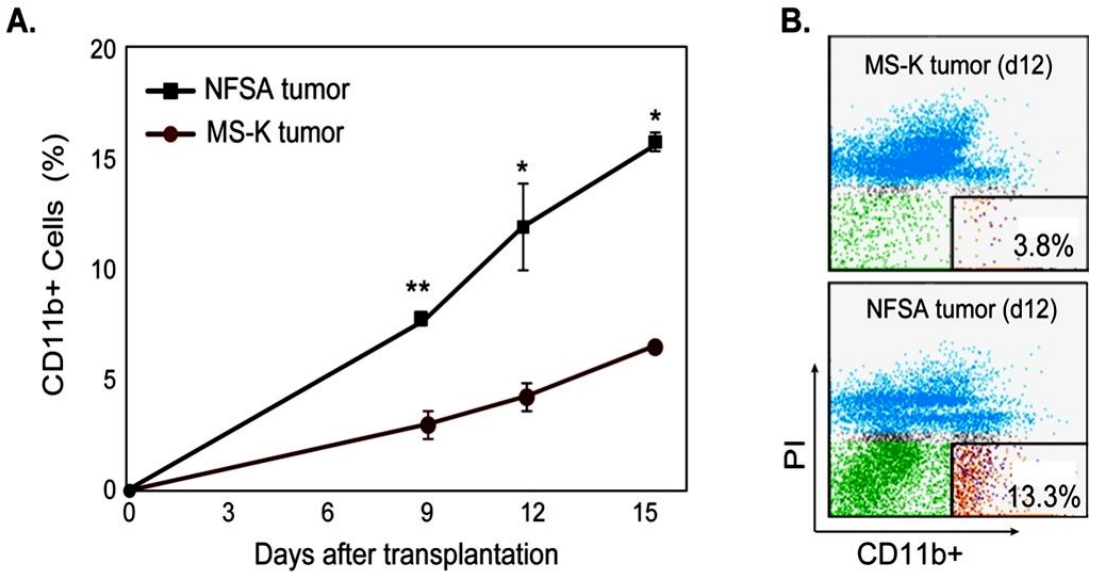

Figure 4. Accumulation of CD11b+ cells in tumor.

A. The accumulation of CD11b+ cells in each tumor. The data were the mean percentages of CD11b+ cells in the tumors (n=3).

B. Scatter diagrams of FACS indicated the CD11b+ cells in MS-K tumor (upper) or NFSA tumor (lower) at day 12. All bars show the mean ± S.E. Asterisks denote significant differences, *: *p<0.05, **: p<0.005*.

3.4 Gene profiles of tumor derived CD11b+ cells

Next, the expression of several M1 macrophage marker genes, including *Nos2*, *IL-6* and *tnf-α*, and M2 macrophage marker genes, including *IL-10* and *Arg-1*, was determined in tumor derived CD11b+ cells. The NFSA tumor derived the CD11b+ cells showed an increased expression of the inflammatory factors, *Nos2*, *tnf-α*, *IL-6*, and decreased expression of *IL-10* according to the tumor progression process (**Fig. 5**). In contrast, the MS-K tumor derived CD11b+ cells displayed a conversed phenotype which down-regulated the expression of *tnf-α*, *IL-6* and up-regulated the expression of *IL-10*. Though there was increased expression of *Nos2* in MS-K tumor derived CD11b+ cells. The expression of *Nos2* was still lower than that in NFSA tumor derived CD11b+ cells. Furthermore, the *arginase-I* (*Arg-1*), a typical M2 marker (4), was not detected in both CD11b+ cell populations (**Fig. 5**).

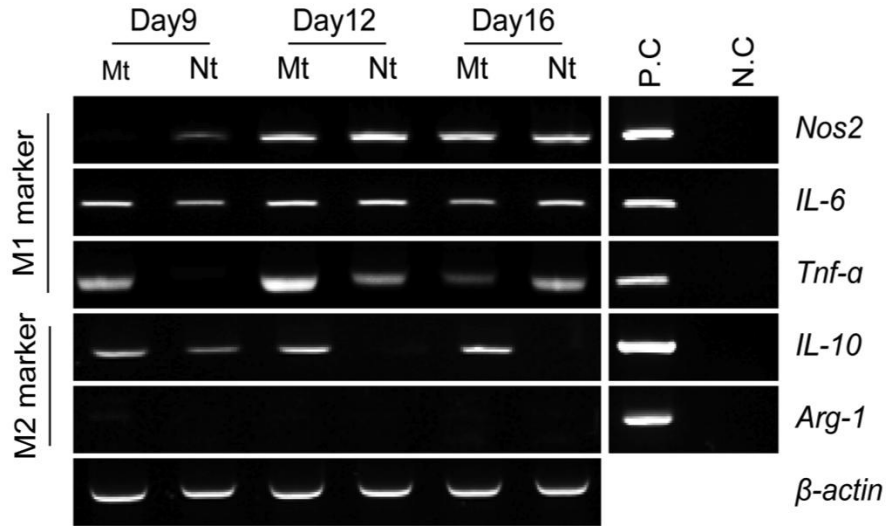

Figure 5. Expression of specific genes in tumor derived CD11b+ cells. Expression of specific genes was analyzed by RT-PCR. *M1 marker*: M1-type macrophage marker, *M2 marker*: M2-type macropahge marker, *Mt*: MS-K tumor-derived CD11b+ cells, *Nt*: NFSA tumor-derived CD11b+ cells, *P.C.*: positive control. *N.C.*: negative control without cDNA template.

3.5 Effect of CM on enhancement of phagocytosis of RAW264 cells

As the most represented leukocytes in cancer tissues, macrophages play critical roles in established tumors progression (53). The phagocytosis in phagocytic cells, especially in macrophages, is a central event of cellular protection, acting to one of the key processes involved in eliminating foreign material or pathogens from an organism, maintenance of tissue homeostasis, as well as in development (54), and is sometimes accompanied by inflammation (55, 56). Therefore, first of all, we examined the effect of CM on the phagocytosis of macrophages. To determine the effect of tumor cells on macrophages, the macrophage cell line, RAW264 cells was used in *in vitro* studies. The phagocytosis analysis revealed that the NFSA-CM enhanced the phagocytosis of RAW264 cells, compared to the no obvious effect in MS-K-CM (**Fig. 6A, B**). Furthermore, the enhancement of phagocytosis in the RAW264 cells by NFSA-CM was dose-dependently (**Fig. 6A**).

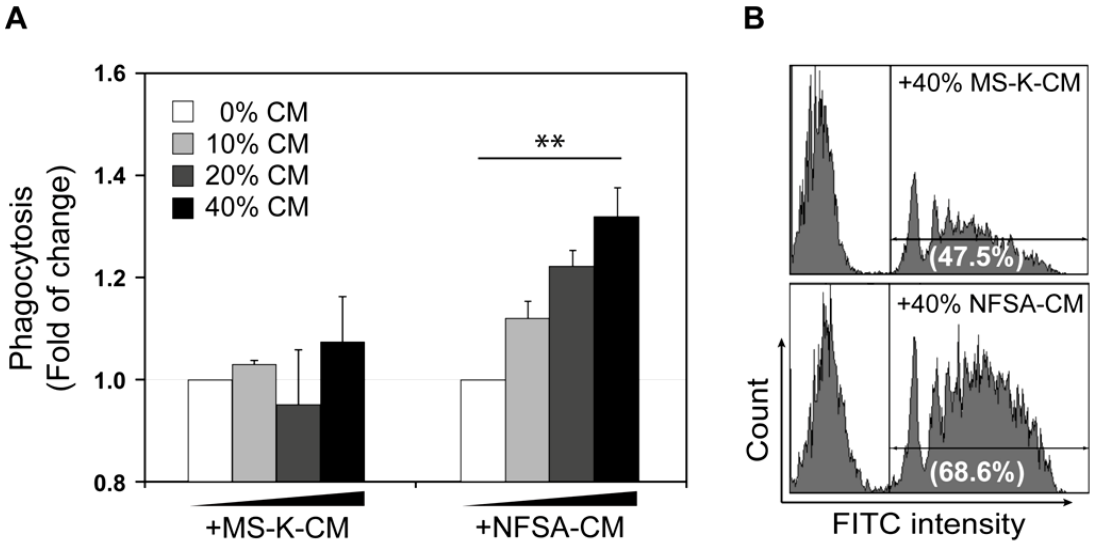

Figure 6. The effect of CM on the phagocytosis of RAW264 cells.
The RAW264 cells were stimulated with various concentration of CM for 5 days. Then the cells were fed with FITC-labeled microshperes. The ratio of FITC-positive cells was determined by FACS.

A. Changes of phagocytosis in RAW264 cells. Results were expressed as the relative pahgocytosis. The relative phagocytosis in the unstimulated RAW264 cells was set to 1.

B. Histogram showed the results of FACS analysis. Number in each panel represented the ratio of FITC+ cells. *+MS-K-CM:* RAW264 cells were treated with MS-K-CM. *+NFSA-CM*: RAW264 cells were treated with NFSA-CM. The details were described in material and methods section.

Asterisks denote significant differences, **: $p<0.005$.

3.6 Effect of CM on polarization of RAW264 cells

To determine the efficiency of CM on polarization of RAW264 cells, the expression of CD80, a typical M1-type macrophages cell surface marker (57), and CD206, one of M2-type macrophages markers (58), was analyzed by FACS. Compared to MS-K-CM, NFSA-CM was more effective for inducing the expression of CD80 in the RAW264 cells (**Fig. 7A**). In contrast, neither NFSA-CM nor MS-K-CM was responsible for inducing the cell surface expression of CD206 (**Fig. 7B**).

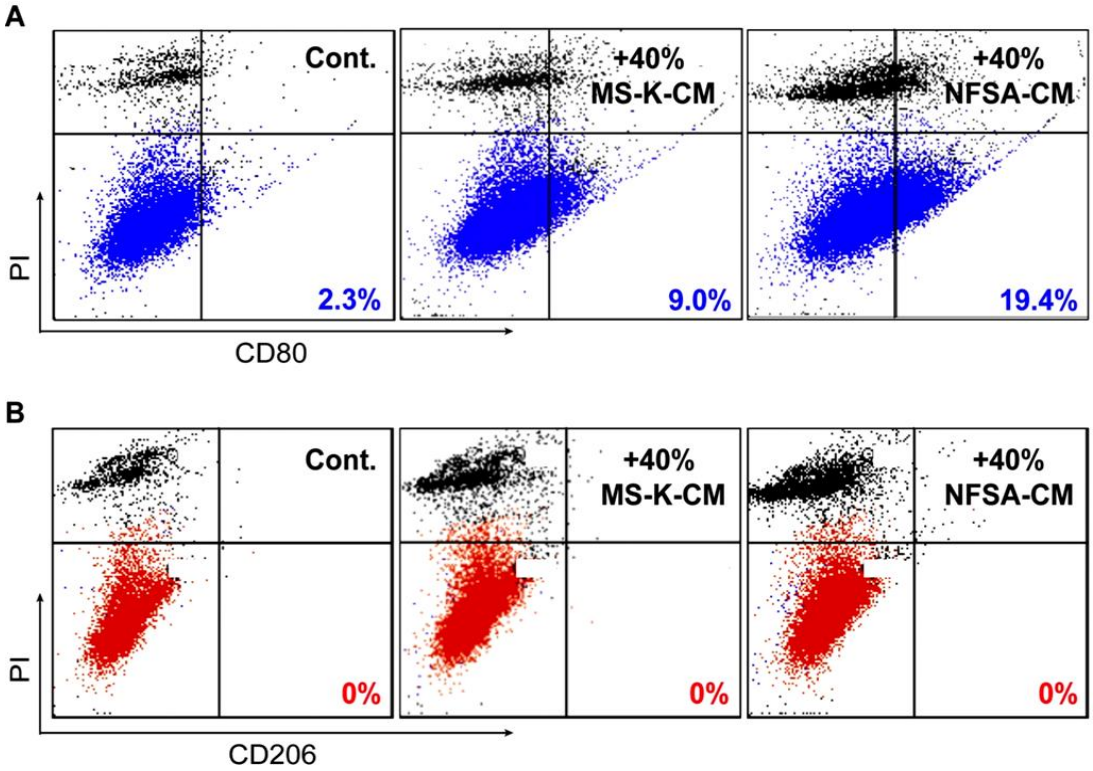

Figure 7. Effect of CM on polarization of RAW264 cells.

The RAW264 cells were stimulated with 40% of MS-K-CM or NFSA-CM (vol/vol) for 5 days. The expression of CD80 and CD206 was analyzed by FACS.

A/B. Scatter diagram shows the results of FACS-analysis. The numbers in upper panels represented CD80-positive cells, and the numbers in lower panels represented the CD206-positive cells. *Cont.*: control, RAW264 cells without treatment. *+40% MS-K-CM*: RAW264 cells were stimulated with 40% of MS-K-CM. *+40% NFSA-CM*: RAW264 cells were stimulated with 40% of NFSA-CM.

It was known that the *Nos2* was one of the hallmark genes of typical M1-type macrophages (59). Expression of this gene was analyzed in the RAW264 cells by real-time PCR. The results showed that NFSA-CM induced the up-regulated expression of *Nos2* in RAW264 cells, but no obvious effect was observed in MS-K-CM treated cells (**Fig. 8**).

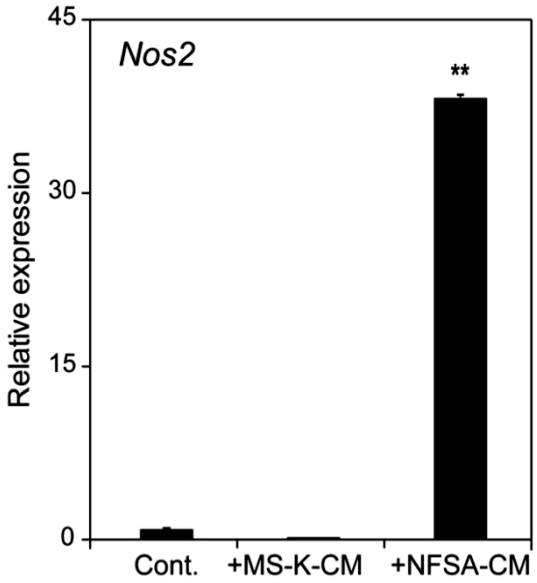

Figure 8. **NFSA-CM induced the expresion of *Nos2*.**

RAW264 cells were treated with 40% MS-K-CM or NFSA-CM for 5 days. Then the relative expression of *Nos2* in RAW264 cells was determined by real-time PCR. The relative expression of the *Nos2* in the MS-K cells was set

to 1. *Cont*.: control RAW264 cells without treatment. *+MS-K-CM*: cells were treated with 40% of MS-K-CM. *+NFSA-CM*: cells were treated with 40% of NFSA-CM. All bars show the mean ± S.E. Asterisks denote significant differences, **: $p<0.005$.

3.7 NFSA cells expressed high-level of *IL-18* and *Casp-1*

To conform the difference in expression of *IL-18* and *Casp-1* in MS-K and NFSA cells, the real-time PCR and semi-quantitative RT-PCR were performed. The results revealed that NFSA cells expresssed higher level of both *IL-18* and *Casp-1*, as well as the microarray data (**Fig. 9 A, B**). It suggeted that the RAW264 cells might be stimulated by the IL-18 which was produced from NFSA cells. Additionally, we checked the expression of *IL-18* and *Casp-1* in MS-K tumors and NFSA tumors by semi-quantitative RT-PCR. The results indicated that NFSA tumor showed a higher experssion of both *IL-18* and *Casp-1* (**Fig. 9 B**).

The level of IL-18 in CM was also determined by ELISA kit. The result revealed that the concentration of IL-18 in NFSA-CM was 179.4±7.8 pg/mL, and that in MS-K-CM was 36.9±16.6 pg/mL (**Fig. 9C**).

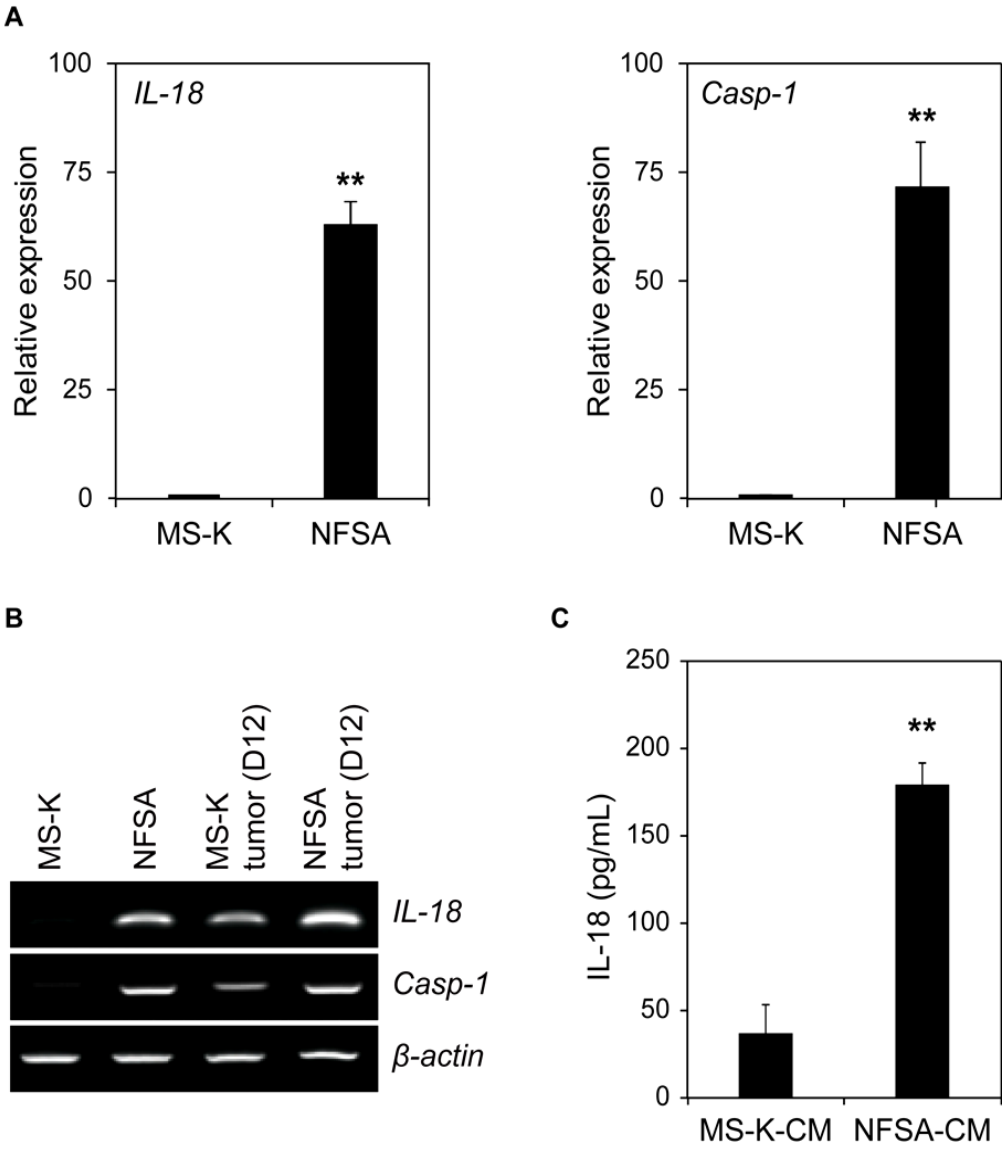

Figure 9. **NFSA cells expressed high-level of *IL-18* and *Casp-1***.

A. Real-time PCR revealed the expression of *IL-18* and *Casp-1* in the MS-K and NFSA cells. The relative expression of each gene in the MS-K cells was set to 1. All bars show the mean ± S.E. Asterisks denote significant differences, **: *p<0.005*.

B. RT-PCR analysis revelaed the expression of the *IL-18* and *Casp-1*.

C. ELISA assay showed the level of the IL-18 in the CM.

All bars show the mean ± S.E. Asterisks denote significant differences, **: *p<0.005*.

3.8 Recombinant IL-18 enhanced the phagocytosis in RAW264 cells

Because the NFSA-CM was responsible for enhancing the phagocytosis in RAW264 cells, effect of recombinant IL-18 (rIL-18) on phagocytosis of RAW264 cells was investigated. Both rIL-18 and NFSA-CM enhanced the phagocytosis in macrophages on day 5 (**Fig. 10A**). Even the NFSA-CM induced the phagocytosis in RAW264 cells on day 1; the performance was not as good as that on day 5. Furthermore, neither rIL-18 nor NFSA-CM was effective for enhancing the phagocytosis in RAW264 cells on day 3 (**Fig. 10A**). After analyzing the phagocytosis on day 5, the cells were loaded on saline coated glass slides using cytospin. Then cells were stained with May-Grünwald-Giemsa solution (**Fig. 10B**). The photographs showed that rIL-18- or NFSA-CM-stimulated RAW264 cells ate much more FITC-labeled microspheres into per cell (**Fig. 10B**). Next, the phagocytosis in the stimulated RAW 264 cells was analyzed (**Fig. 11**). Various concentration of rIL-18 (0 to 10ng/mL) or the NFSA-CM was used for stimulation. The IL-18 enhanced the phagocytosis of the RAW264 cells in a dose-dependent manner. Furthermore, the heat-inactivated NFSA-CM was also effective for enhancing the phagocytosis in RAW264 cells (**Fig. 11**). Thus, the complement system was excluded from this phenomenon.

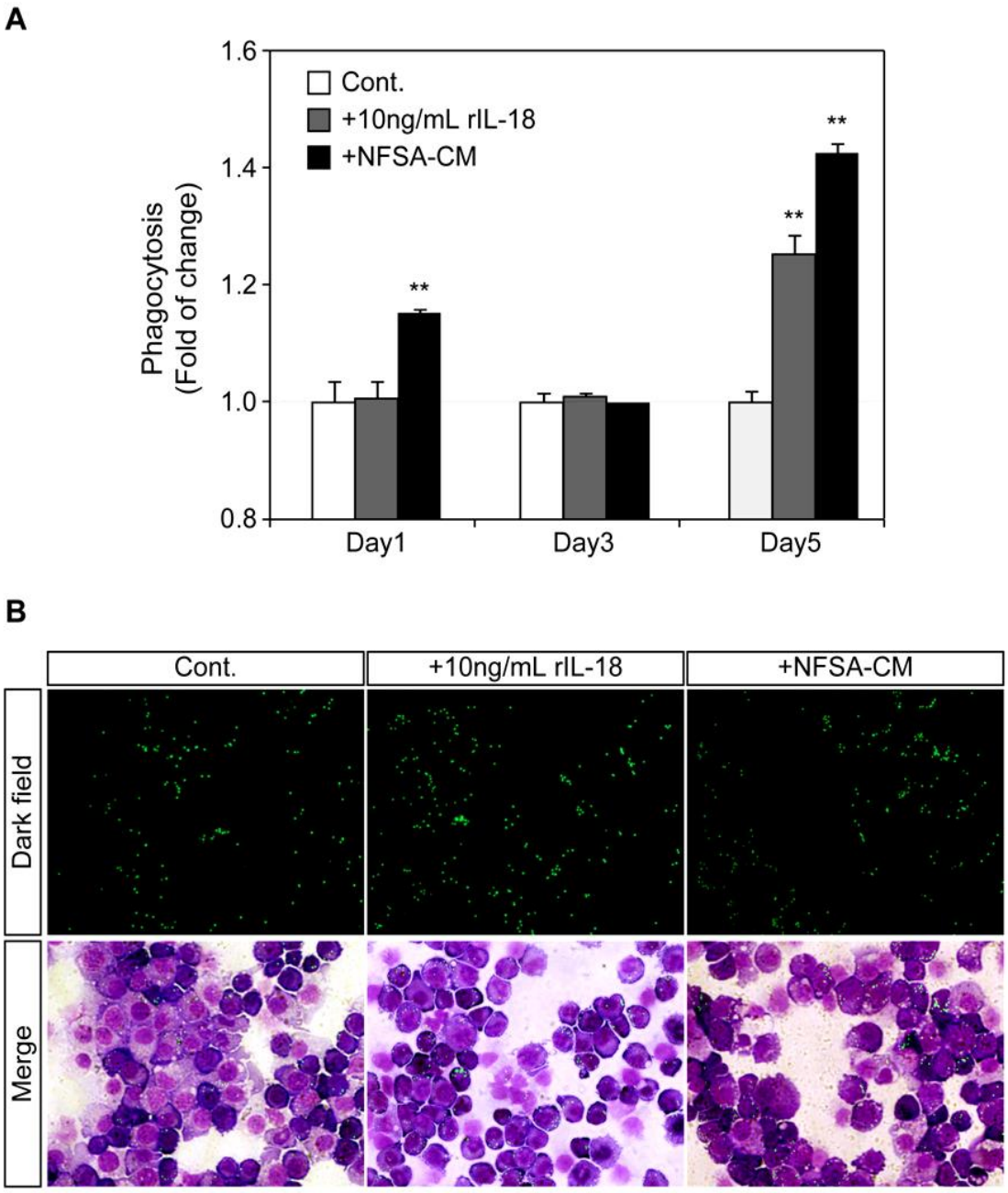

Figure 10. **Recombinant IL-18 enhanced the phagocytosis of RAW264 cells.**

A. RAW264 cells were treated with 40% NFSA-CM or 10 ng/mL of rIL-18 for 1 day, 3 days or 5 days. Then phagocytosis was analyzed by FACS. Results are expressed as relative pahgocytosis. The relative pahgocytosis in untreated RAW264 cells was set to 1. *Cont.*: control, cells without stimulation. All bars show the mean ± S.E. Asterisks denote significant differences, **: $p<0.005$.

B. Cytospin slides were prepared from cultured cells on day 5, cells were stained with May-Grünwald-Giemsa and photographs were taken by fluorescence microscopy. Upper panel showed photographs in dark field. Lower panel showed merged images. Original magnification X20.

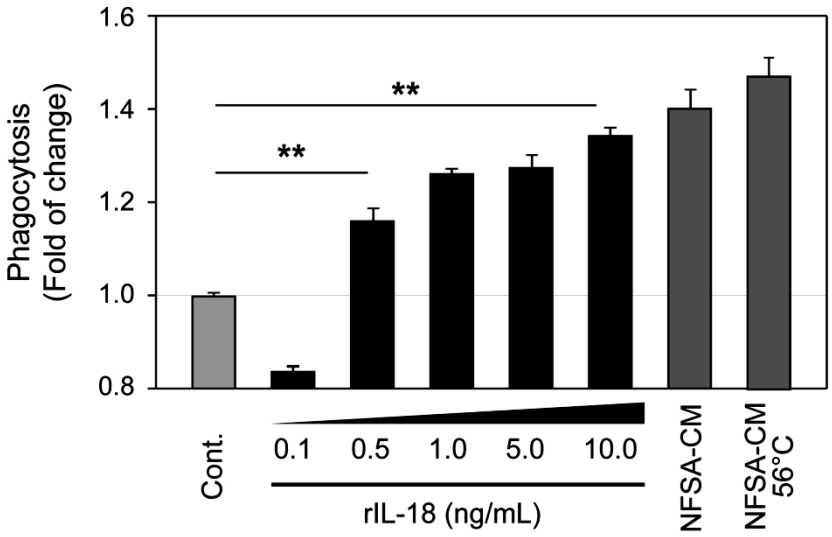

Figure 11. **Recombinant IL-18 enhanced the phagocytosis of RAW264 cells in a dose-dependent manner.**

RAW264 cells were treated with various concentration of rIL-18 for 5 days. The phagocytosis was analyzed by FACS. Results are expressed as the relative pahgocytosis. The relative pahgocytosis in untreated RAW264 cells was set to 1. *Cont.*: control, cells without treatment. All bars show the mean ± S.E. Asterisks denote significant differences, **: *p<0.005*.

3.9 IL-18 was the key factor in NFSA-CM for promoting phagocytosis in RAW264 cells

To evaluate the involvement of IL-18 on phagocytosis of macrophages, the neutralizing anti-IL18 antibody was used. The cells were treated with rIL-18 or NFSA-CM with or without anti-IL18 antibody (α-IL-18Ab) for 5 days. Then the phagocytosis was analyzed by FACS.

The results showed that the uptake of microspheres was inhibited completely by the αIL-18Ab (**Figure 12**). These results suggested that a

direct effect of exogenous IL-18 on enhancement of phagocytosis in RAW264 cells. Therefore, IL-18 was one of the critical effectors in the NFSA-CM which enhanced the phagocytosis.

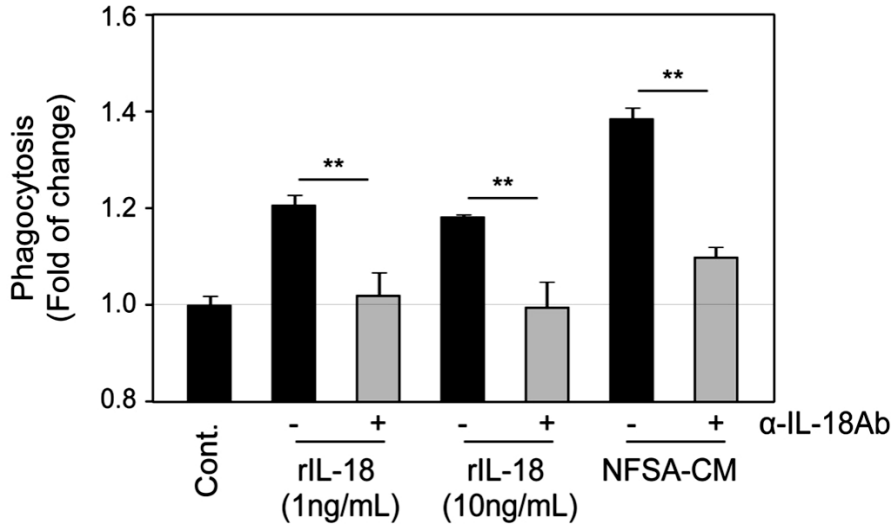

Figure 12. Anti-IL-18 antibody inhibited phagocytosis in the rIL-18- or NFSA-CM-stimulated RAW264 cells.

Phagocytosis was determined on RAW264 cells exposed to rIL-18 or NFSA-CM and in the presence of the neutralizing anti-IL-18 antibody (αIL-18Ab). Final concentration of the α-IL-18Ab was 1 μg/mL. Results are expressed as the relative pahgocytosis. The relative pahogocytosis in un-stimulated RAW264 cells was set to 1. *Cont.*: control, cells without treatment. *αIL-18Ab*: neutrilizing antibody to IL-18. All bars show the mean ± S.E. Asterisks denote significant differences, **: $p<0.005$.

3.10 Recombinant IL-18 enhanced the phagocytosis in primary macrophages

To investigate whether the IL-18 was also effective for enhancing the phagocytosis in native macrophages or not, the peritoneal macrophages were separated from murine abdominal adherent cells. The purified CD19-negative macrophages were used. The results indicated that the

phagocytosis was up-regulated by both rIL-18 and NFSA-CM, and that was inhibited by the αIL-18Ab (**Fig. 13**). These data revealed a critical effect of NFSA derived IL-18 on the enhancement of phagocytosis in native primary macrophages.

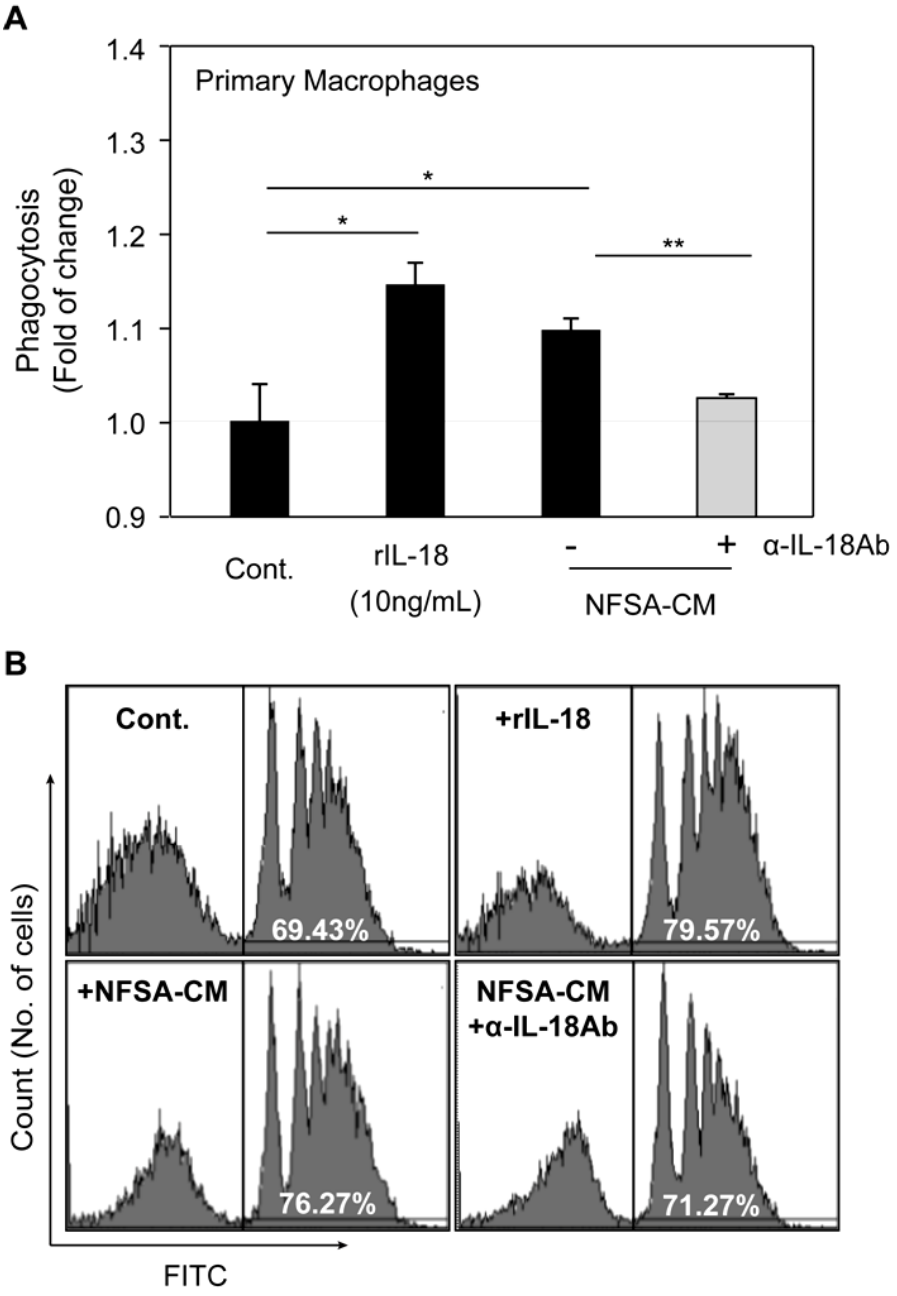

Figure 13. Recombinant IL-18 enhanced the phagocytosis in murine primary macrophages.

The primary macrophages were stimulated with 10 ng/mL of rIL-18 or 40% of NFSA-CM for 5 days. The neutralizing anti-IL-18 antibody (αIL-18Ab) was added at a final concentration as 5 μg/mL. Phagocytosis was analyzed by FACS.

A. Effect of rIL-18 on phagocytosis of peritoneal macrophages. The relative phagocytosis was in un-stimulated RAW264 cells was set to 1. All bars show the mean ± S.E. Asterisks denote significant differences, **: $p<0.005$.

B. Histogram presents the results of FACS analysis. Number in each panel presented the percentage of FITC+ cells. *Cont.*: control, cells without treatment. *αIL-18Ab*: neutrilizing antibody against IL-18.

3.11 Polarization of RAW264 cells by IL-18 wasn't associated to the induction of *IFN-γ*.

Since the data suggested that the existence of M1-type macrophages in NFSA-CM-stimulated RAW264 cells, the characters of rIL-18 stimulated RAW264 cells was analyzed. The expression of several pro-inflammation- and anti-angiogenesis-related factors (that is M1-type macrophage markers), including *Nos2*, *IL-6* and *tnf-*α (60, 61) and the anti-inflammation factors (that is M2-type macrophage markers), *IL-10* and *Arg-1* in rIL-18- or NFSA-CM-stimulated RAW264 cells was detected (**Fig. 14**).

The results indicated the up-regulation of M1-markers, *Nos2, IL-6* and *tnf-α* in the RAW264 cells, which were stimulated with rIL-18 or NFSA-CM. The expression of M2-markers, *IL-10* and *Arg-1*, was down regulated by rIL-18 and NFSA-CM in RAW264 cells (**Fig. 14**).

Furthermore, neither rIL-18 nor NFSA-CM induced the expression of *IL-12p40* (**Fig. 15A**), which was a subunit of *IL-12p70*, in stimulated RAW264 cells. Interestingly, after the stimulation with rIL-18 or NFSA-CM for 5 days, the expression of *IFN-γ* was not induced in RAW264 cells, contrarily, it was decreased significently (**Fig. 15B**). In further, addition of IL-18 didn't affect the expression of the receptors, *IL-18r1* and *IL-18rap* (**Fig. 15A**).

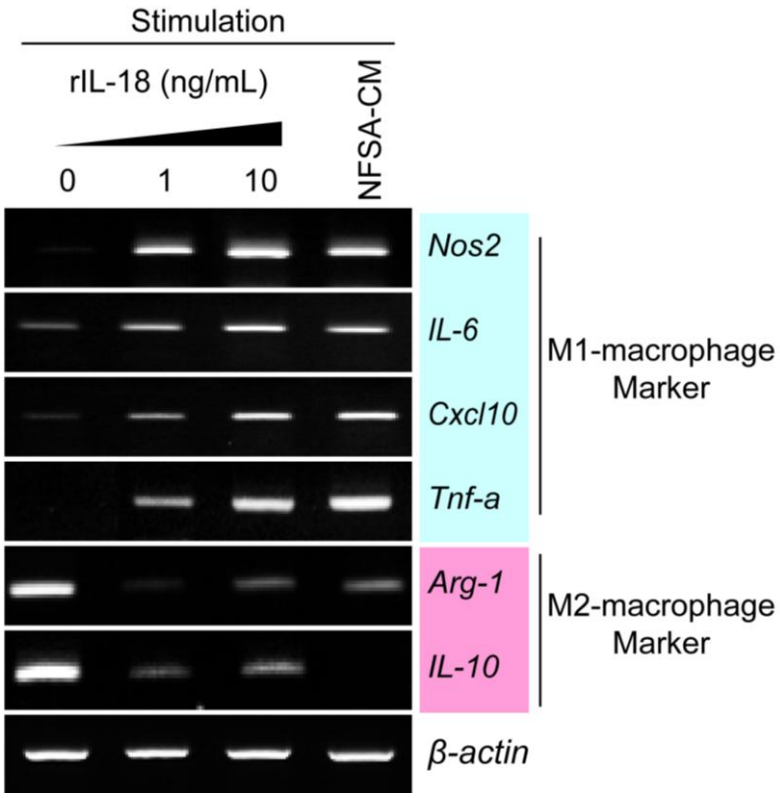

Figure 14. Effect of rIL-18 and NFSA-CM on the acquisition of M1- and lossing of M2-specific markers in RAW264 cells.
The expression of *Nos2*, *IL-6*, *Cxcl10*, *tnf-α*, *Arg-1* and *IL-10* in IL-18-stimulated RAW264 cells was analyzed by RT-PCR. Blue box indicated the M1-type macrophages specific markers (M1 marker). Pink box indicated the M2-type macrophages specific markers (M2 marker). *β-actin* was used as control.

More interestingly, the induction of the *Nos2* was induced by IL-18 alone in this experiment (**Fig. 14**) and the expression of the *IFN-γ* was not induced (**Fig. 15B**), though Heike et al. have reported that the induction of *Nos2* in murine peritoneal macrophages was induced by stimulation with the combination of IL-18 and IL-12 for 48hr and that process was mediated by *IFN-γ* (46). Since the expression of the *IL-12p40* was not detected in IL-18-stimulated RAW264 cells, it indicated that the IL-12 was not produced

from RAW264 cells itself. The bioactive IL-12 is produced as the heterodimer of the IL-12p35 and IL-12p40 (62).

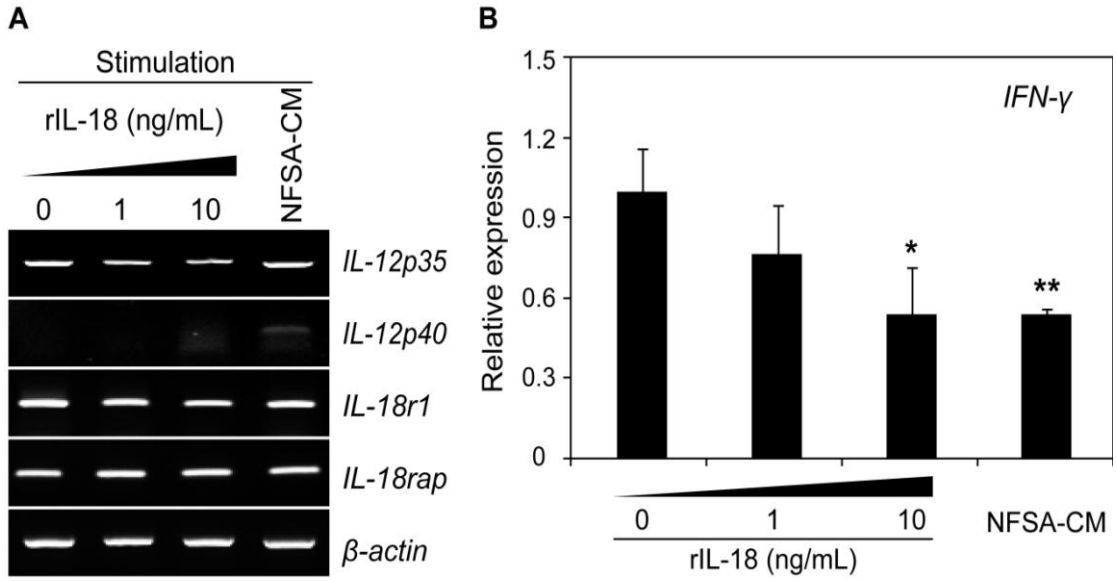

Figure 15. IL-18 alone induced the polarization of RAW264 cells independently to *IFN-γ*.

A. The expression of specific genes in the IL-18-stimulated RAW264 cells was analyzed by RT-PCR.

B. Quantitative-PCR analysis of the expression of *IFN-γ* in the RAW264 cells. The RAW264 cells were stimulated with rIL-18 or NFSA-CM for 5 days. The relative expression of *IFN-γ* in the unstimulated RAW264 cells was set to 1. All bars showed the mean ± S.E. Asterisks denote significant differences, *: $p<0.05$, **: $p<0.005$.

3.12 IL-18 contributed to the polarization of murine primary macrophages.

Next, the contribution of the NFSA-CM and IL-18 on polarization of native macrophages was investigated. The expression of the M1-marker genes was analyzed in the IL-18- or NFSA-CM-stimulated primary macrophages (**Fig. 16**). The results indicated that both rIL-18 and NFSA-CM

induced the expression of the M1-marker genes, including *Nos2*, *IL-6* and *tnf-α*. But no detectable expression of M2-marker genes, including *IL-10* and *Arg-1* in the IL-18- or NFSA-CM-stimulated macrophages was observed (**Fig. 16**). Contrary to this, the MS-K-CM induced the expression of *IL-10*, without induction of the *Nos2*, *IL-6* and *tnf-α*. The neutralizing anti-IL-18 antibody (αIL-18Ab) suppressed the expression of *Nos2*, *IL-6* and *tnf-α*, with enhanced expression of *IL-10* in NFSA-CM-stimulated primary macrophages (**Fig. 16**). However, the neither rIL-18 nor NFSA-CM was effective for inducing the expression of *Cxcl10* in primary macrophages. Even this gene was up-regulated in RAW264 cells by rIL-18 and NFSA-CM (**Fig. 16**). These data revealed a critical effect of IL-18 in NFSA-CM on polarization of primary macrophages.

In addition, the expression of *IL-12p35* and *IL-12p40* in primary macrophages was also analyzed. The RT-PCR results showed that neither *IL12p35* nor *IL-12p40* was up-regulated by stimulation (**Fig. 17**). There was extremely low level expression of *IL12p35* in IL-18- or MS-K-CM stimulated primary macrophages. Therefore, these data indicated that IL-18 alone contributed to program the primary macrophages to express M1-markers, and the IL-18 was the one of the key effectors in NFSA-CM for inducing the polarization of primary macrophages. Furthermore, the IL-18-stimulation didn't affect the expression of the receptors, *IL-18r1* and *IL-18rap* in the macrophages. Interestingly, the α-IL-18 mediated blockage of IL-18 reduced the expression of *IL-18r1*. It suggested that IL-18 might be important for supporting the expression of *IL-18r1* (**Fig. 17**).

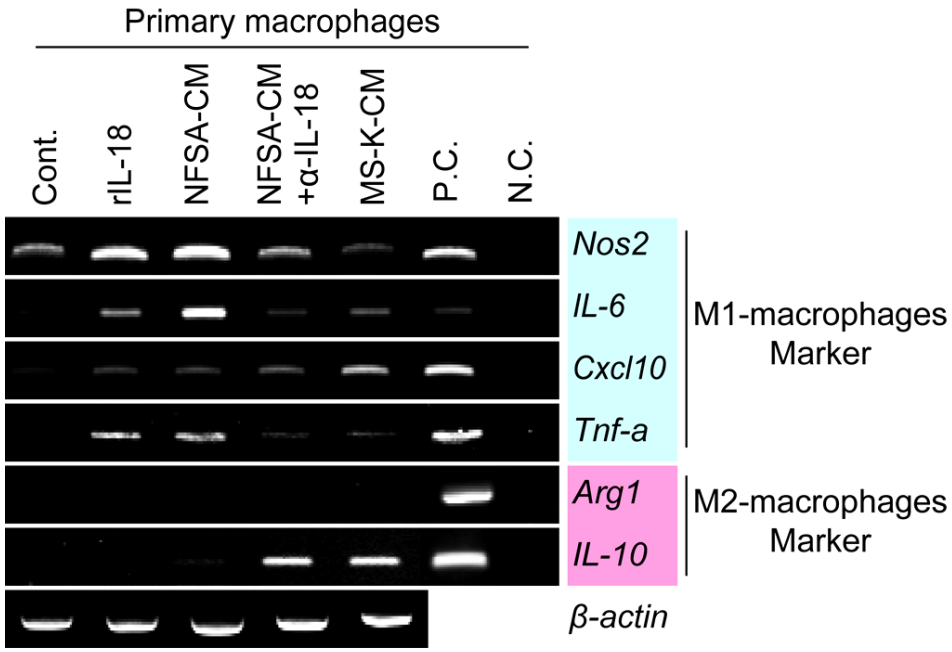

Figure 16. Effect of rIL-18 and NFSA-CM on the acquisition of M1-markers in murine primary macrophages.

The expression of *Nos2*, *IL-6*, *Cxcl10*, *tnf-α*, *Arg-1* and *IL-10* was analyzed by RT-PCR in rIL-18- or NFSA-CM-stimulated macrophages. The neutrilazing anti-IL-18 antibody (αIL-18Ab) was used at a final concentration as 5μg/mL. Blue box indicates the M1-type macrophages specific markers (M1 Marker) and pink box indicates the M2-type macrophages specific markers (M2 Marker), respectively. *β-actin* was used as control. *Cont.*: control, primary macrophages without stimulation. *P.C.*: positive control, plasmid was used as the template DNA. *N.C.*: negative control, without template.

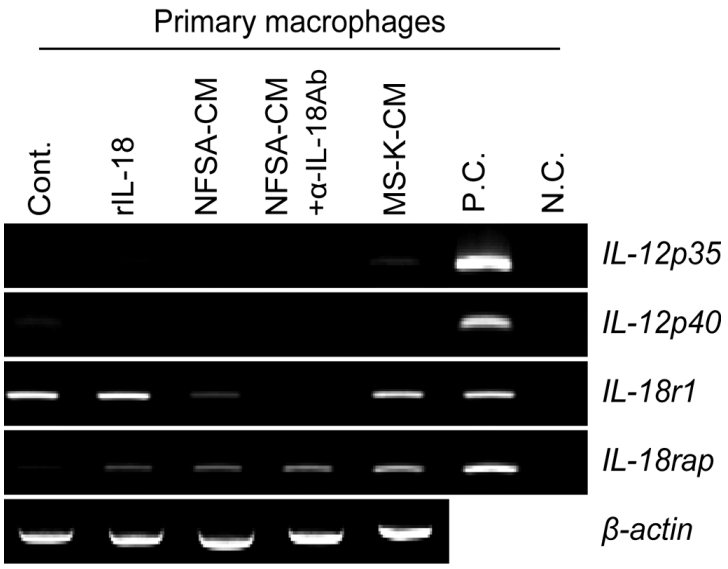

Figure 17. IL-18 alone induced the polarization of primary macrophages.

The expression of *IL-12p35*, *IL-12p40*, *IL-18r1* and *IL-18rap* in primary macrophages was analyzed by RT-PCR. *β-actin* was used as control. The αIL-18Ab was used at a final concentration of 5 μg/mL. *Cont.*: control, primary macrophages without stimulation. *P.C.*: positive control, plasmid was used as the template DNA. *N.C.*: negative control, without template.

3.12 Enhanced cytotoxicity of IL-18 stimulated RAW264 cells to endothelial cells

The M1-marker positive macrophage played an important role on protecting the host from infection and tumors by preventing angiogenesis (4). As the essential cellular components of blood vessels, endothelial cells played critical role in new blood vessels formation (63, 64). Thus, the influence of the IL-18- or NFSA-CM stimulated RAW264 cells on survival of endothelial cells *in vitro* was assayed.

Firstly, the direct co-culture of stimulated RAW264 cells and endothelial cells, F-2-Orange, was performed (**Fig. 18A**). The survival ratio of F-2-Orange was drastically reduced by the direct co-culture with the

stimulated RAW264 cells (**Fig. 18B**). Furthermore, the damaging ratio was severely dependent on the number of the stimulated RAW264 cells (**Fig. 18C**).

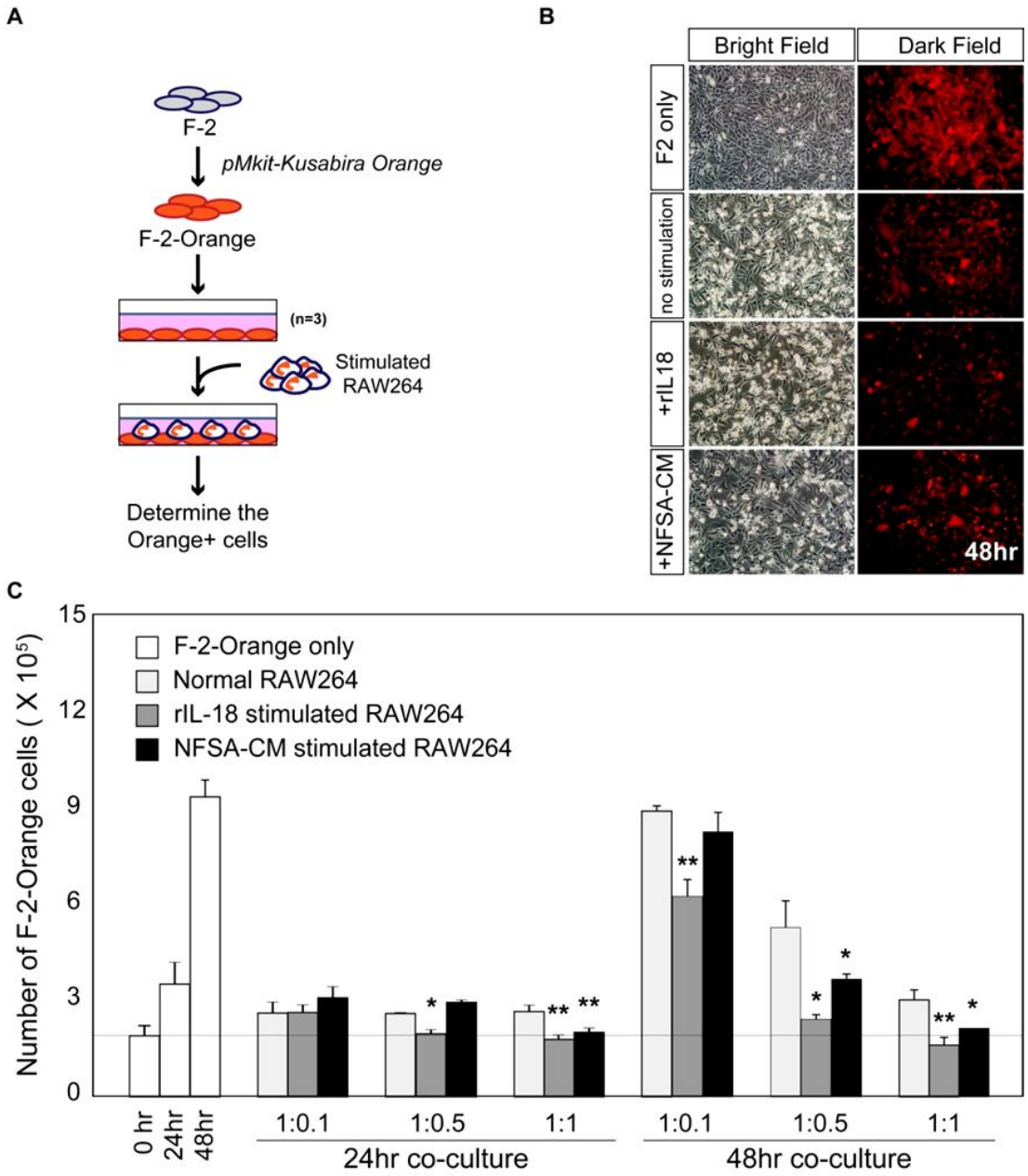

Figure 18. Damage of F-2-Orange cells by rIL-18- or NFSA-CM-stimulated RAW264 cells.

A. The schema of the experiment. Co-culture was performed in 35mm dishes.

B. The photographs show the co-cultured cells at 48 hours. After co-culture, cells were visualized by fluorescent microscopy. The left panels show the phase contrast images, and the right panels show the fluorescent images. Original magnification was X20.
C. The histogram shows the number of surviving F-2-Orange cells after 24 or 48 hours of direct co-culture with stimulated RAW264.7 cells. The number of F-2-Orange cells was determined by FACS. Non-stimulated RAW264 cells were used as a control. All bars show the mean ± S.E, n=3. Asterisks denote significant differences, *: *p<0.05,* **: *p<0.005*.

3.13 Enhanced cytotoxicity to endothelial cells in RAW264 cells via soluble mediators

To investigate whether the direct cell-to-cell contact was necessary for damaging the endothelial cells or not, the membrane-separated co-culture was carried out in 6-well Transwell plates. The F-2-Orange cells were plated at a proper density in the lower chamber of the transwell plates to make a monolayer. After 24hours of pre-incubation, the stimulated RAW264 cells were plated into the upper chamber of the transwell plates, and were co-cultured for 48hours (**Fig. 19A**). After 48 hours of co-culture, the number of surviving F-2-Orange cells decreased significantly (**Fig. 19B, C**).

These results clearly indicated that some soluble factors that were produced from the stimulated RAW264 cells must function in the killing of the F-2-Orange cells. However, compared to the direct co-culture assay (Figure 18C, F-2-Orange : RAW264 = 1:1), the F-2-Orange cells were damaged less severely by membrane-separated co-culture (**Fig. 18C, 19C**). This result suggested that the direct cell-to-cell interaction between IL-18- stimulated macrophages and endothelial cells may play a critical role in damaging endothelial cells, in addition to soluble factors secreted from IL-18-stimulated macrophages.

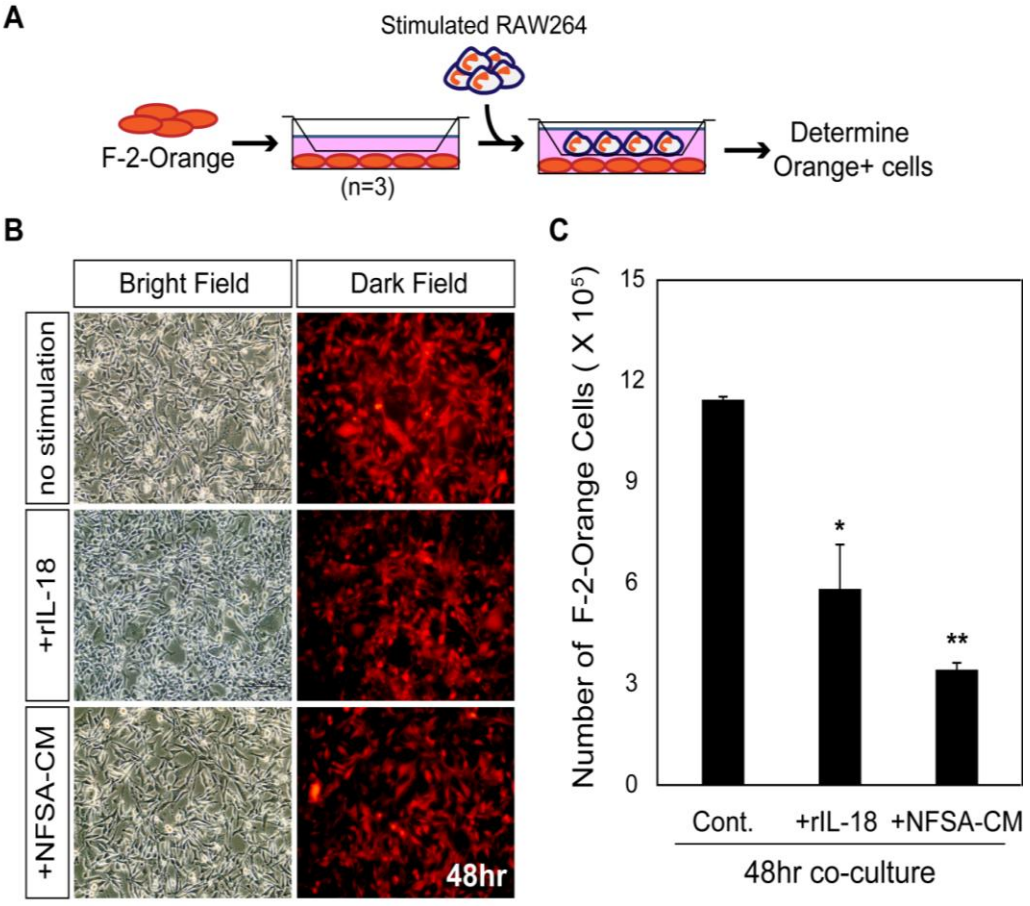

Figure 19. Enhanced cytotoxicity to F-2-Orange cells in IL-18- or NFSA-CM-stimulated RAW264 cells.

A. Scheme of a transwell co-culture assay system. Ratio between F-2-Orange cells and RAW264 cells was set as 1:1. The co-culture was performed in 6-well transwell plates.

B. The photographs showed the surviving F-2-Orange cells at 48 hours. The left panels showed the phase contrast images, and the right panels showed the fluorescent images.

C. The histogram shows the number of surviving F-2-Orange cells after 48 hours co-culture. The number of surviving F-2-Orange cells was indicated. Non-stimulated RAW264 cells were used as a control. All bars show the mean ± S.E, n=3. Asterisks denote significant differences, *: *p<0.05,* **: *p<0.005*.

3.14 1400w abolished the enhanced cytotoxicity to endothelial cells in RAW264 cells

The PCR results demonstrated the increased expression of *Nos2*, the predominant generator of NO (65), in IL-18- or NFSA-CM-stimulated RAW264 cells (Figure 8&14). We investigated whether the NOS2-genarated NO was responsible for the damaging of F-2-Oranges cells or not. The inhibitor of NOS2, 1400w (21), was used in the Transwell co-culture system.

The results revealed that the enhanced cytotoxicity of the stimulated RAW264 cells was abolished by the NOS2 inhibitor 1400w (**Fig. 20 B & C**). These results clearly demonstrated that rIL-18 and NFSA-CM stimulate RAW264 cells to damage the endothelium and that some soluble components, such as NO, secreted from the stimulated RAW264 cells damaged the F-2-Orange cells in our assay.

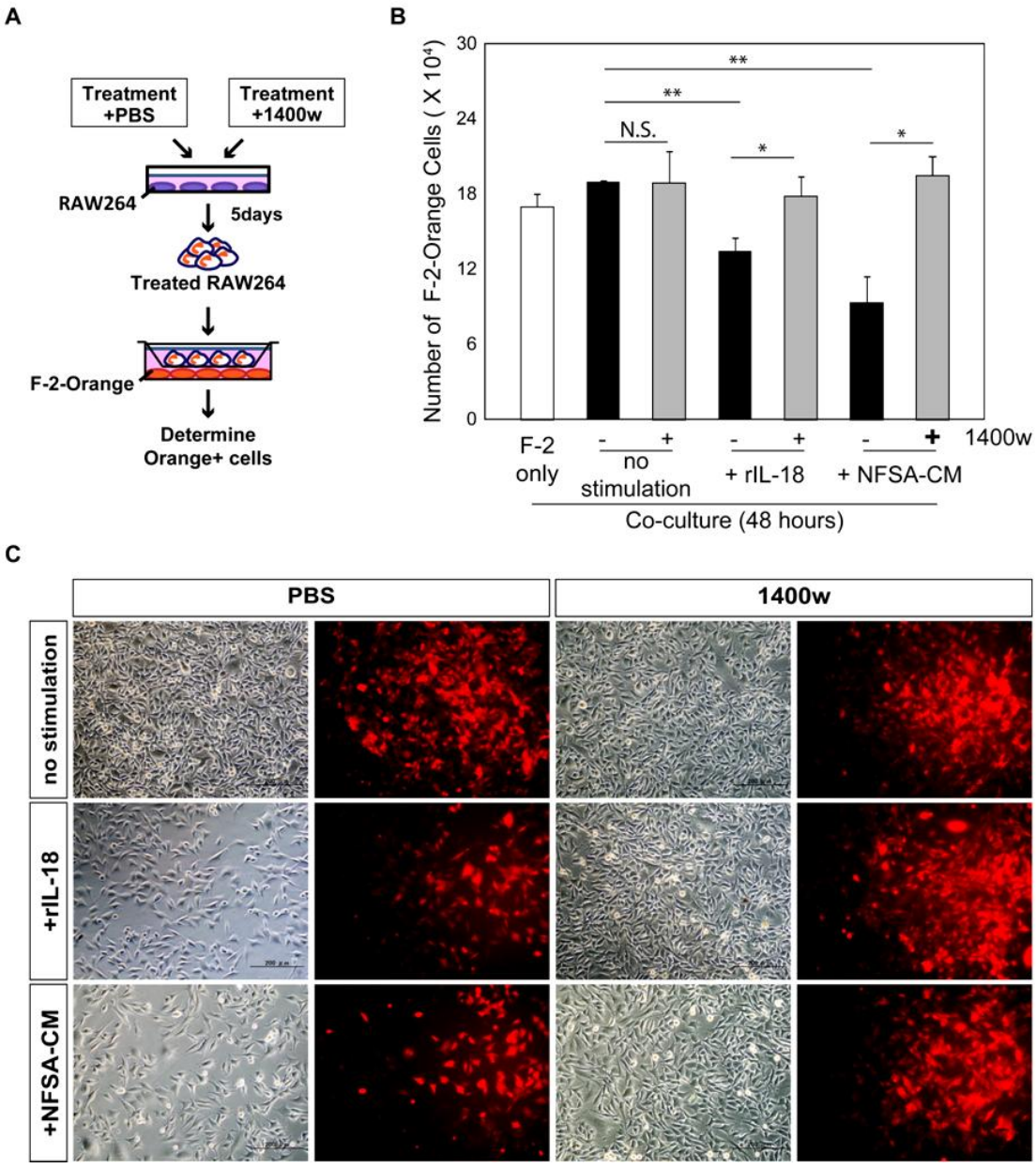

Figure 20. 1400w abrogates the enhanced cytotoxicity to F-2-Orange cells in IL-18- or NFSA-CM-stimulated RAW264 cells.

A. Scheme of a transwell co-culture assay system. The co-culture was performed in 24-well transwell plates.

B. The histogram shows the number of surviving F-2-Orange cells after 48 hours co-culture. The number of surviving F-2-Orange cells was indicated. Effect of the NOS2 inhibitor (1400w) was also analyzed. Non-stimulated RAW264 cells were used as a control in all experiments. All bars show the mean ± S.E, n=3. Asterisks denote significant differences, *: *p<0.05,* **: *p<0.005*, N.S.: not significant.

C. The photographs showed the surviving F-2-Orange cells at 48 hours. The left panels showed the phase contrast images, and the right panels showed the fluorescent images, with or without the 1400w.

Table 1. Comparison of gene expression in NFSA and MS-K

Gene		Accession No.	Signal		Log2 ratio (NFSA/MS-K)
			NFSA	MS-K	
Chemokine ligand	*chemokine (C-C motif) ligand 11 (Ccl11)*	NM_011330	9.13E+03	6.15E+00	10.54
	chemokine (C-C motif) ligand 8 (Ccl8)	NM_021443	1.49E+04	2.28E+02	6.03
	chemokine (C-C motif) ligand 7 (Ccl7)	NM_013654	1.86E+05	3.00E+03	5.95
	chemokine (C-X-C motif) ligand 3 (Cxcl3)	NM_203320	3.72E+02	7.85E+00	5.57
	chemokine (C-C motif) ligand 2 (Ccl2)	NM_011333	4.05E+05	1.22E+04	5.05
Cytokine	*interleukin 18 (IL-18)*	NM_008360	1.96E+03	5.90E+01	5.06
	vascular endothelial growth factor-A (Vegfa)	NM_00102525	3.28E+03	7.29E+03	-1.15
Enzyme	*caspase 1 (Casp1)*	NM_009807	2.77E+04	3.34E+01	9.7
Colony stimulating factor	*colony stimulating factor 1 (macrophage) (Csf1)*	NM_007778	2.17E+04	1.23E+04	0.82
	colony stimulating factor 2 (granulocyte-macrophage) (Csf2)	NM_009969	1.29E+01	1.71E+01	-0.41
	colony stimulating factor 3 (granulocyte) (Csf3)	NM_009971	1.16E+02	6.88E+00	4.07

Expression of genes in NFSA and MS-K was analyzed by SurePrint G3 (mouse). Table represents part of the data.

Signal means expression level of each gene in NFSA or MS-K. Log2 ratio means the relative expression of each gene in NFSA against in MS-K.

Table 2. List of primers for genes

Gene	Accession	Sense primer	Anti-sense primer	Tm	Product Size (bp)
IL-18	NM_008360	ATCAAAGTGCCAGTGAACCC	TCAGGTGGATCCATTTCCTC	60	160
Casp-1	NM_009807	GATGGCACATTTCCAGGACT	TCAACTTGAGCTCCAACCCT	60	188
Nos2	NM_010927	TCACCTTCGAGGGCAGCCGA	TCCGTGGCAAAGCGAGCCAG	60	286
IL-6	NM_031168	GCACTTGCAGAAAACAATCTG	TCTGAAGGACTCTGGCTTTGT	54	187
Cxcl10	NM_021274	AAAGTAACTGCCGAAGC	AGAACTGACGAGCCTGA	60	182
tnf-α	NM_013693	GGTTCTGTCCCTTTCACTCA	AGCCATAATCCCTTTCTAA	55	892
IL-12p35	NM_001159424	GCCAGGTGTCTTAGCCAGTC	AGCTCCCTCTTGTTGTGGAA	60	226
IL-12p40	NM_008352	ATGAGAACTACAGCACCAGCTTC	ACTTGAGGGAGAAGTAGGAATGG	62	156
IL-18r1	NM_008365	GCATTCTCATTGTTAAAAGTGCC	CAAGGTGTGATCATGAAAAGTGA	60	221
IL-18rap	NM_010553	ACATATTCTGCAAGGGGTGC	TATGCAGCATGCCTTCACTC	60	241
Arg-1	NM_007482	AACTCAACGGGAGGGTA	CTGGGATACATACTTACTGGA	55	193
IL-10	NM_010548	ACATACTGCTAACCGACTCCT	ACTCTTCACCTGCTCCACT	63	245
β-actin	NM_007393	CAGGGTGTGATGGTGGGAATGGG	CAGGATGGCGTGAGGGAGAGCA	60	408

PCR primers for each gene were listed.

Discussion

As a predominant population of inflammatory cells presented in solid tumors, there is growing evidence indicated that the phenotype of macrophages is dependent on the stages of tumor progression (4). Tumor cells secret a wide spectrum of soluble factors, attracting circulating monocytes to tumor sites and promoting their differentiation to macrophages while blocking differentiation to dendritic cells (DCs) (66). At the early stage of tumor development, blood peripheral monocytes recruited to the tumor mass and differentiated into classically activated phenotype (M1-type) because of the pro-inflammatory tumor microenvironment (53). At the late stage of malignancy transformation, infiltrated macrophages are driven to display an alternatively activated phenotype (M2-type) (53) with reduced iNOS and TNF-α expression (67) by the signals from the tumor and the stroma cells (68), and provide an immunosuppressive microenvironment for tumor growth and promoting angiogenesis (7, 69).

However, the tumorigenesis studies indicated that the tissue necrosis was observed in NFSA tumors (**Fig. 3A, B**). The accumulation of CD11b+ cells in tumors increased with tumor growth. More importantly, in NFSA tumors, more CD11b+ cells were recruited than MS-K tumor (**Fig. 4**). Furthermore, the CD11b+ cells in NFSA tumor showed increased expression of pro-inflammatory factors, *Nos2*, *IL-6* and *tnf-α.* Meanwhile, the expression of immune-suppressive factor, *IL-10* was reduced during the tumor progression. Expression of *Arg-1* was not detected (**Fig. 5**). The phagocytosis of macrophages, which were stimulated by factors produced from NFSA cells but not MS-K cells, was enhanced (**Fig. 6**) and expression of CD80 (**Fig. 7**) was also enhanced, in addition to high expression of *Nos2* (**Fig. 8**). These results suggested the remarkable existence of the immunosupportive M1-type population in macrophages stimulated by the factors produced from NFSA cells. NFSA cells have shown high expression of *IL-18* (**Fig. 9, Table 1.**), and furthermore, DNA microarray analysis has revealed a differential expression

profile of CC-type chemokines in NFSA cells (**Table 1**), which are reported as non-redundant factors in carcinogenesis (70).

In contrast, the concept that IL-18 exerts significant anti-tumor activity is well established (36, 37). This concept drove me to investigate the effect of IL-18 on macrophages, a core effector in tumors. As a central event of cellular protection, phagocytosis in phagocytic cells acts to eliminate foreign material and is sometimes accompanied by inflammation (55, 56). Therefore, the effect of NFSA-CM and IL-18 on the phagocytic activity of macrophages was examined. The results demonstrated that both NFSA-CM and rIL-18 dramatically promoted phagocytosis in both RAW264 cells in a dose dependent manner (**Fig. 6, 10, 11**). Because the complement system in serum is important for identifying “non-self” particles and triggering phagocytosis in macrophages (71, 72), the effect of heat-inactivated NFSA-CM on RAW264 was also examined. The results revealed that the heat-inactivated CM was still effective for enhancing the phagocytosis of RAW264 cells (**Fig. 11**). Thus, it suggests that the effect of NFSA-CM was not associated with the components of the complement system. Lewis et al. showed that the sulforaphane-stimulated phagocytosis of microbeads by RAW264 cells was completely abolished when the cells are cultured in complete medium containing 10% FBS (56). However, in this study, the stimulation of phagocytosis by IL-18 was not abolished by a high concentration of serum. The enhanced phagocytosis was also observed in murine primary macrophages (CD19-negative peritoneal cells) by treating the cells with NFSA-CM or rIL-18 for 5 days (**Fig. 13**). In addition, the presence of neutralization antibody to IL-18 significantly reduced the phagocytosis of the IL-18- or NFSA-CM-stimulated RAW264 cells (**Fig. 12**) and primary macrophages (**Fig. 13**). These results indicate that IL-18 is one of the critical factor in NFSA-CM which enhancing the phagocytosis of microspheres. Consequently, the data indicates that IL-18 exerts a strong effect on enhancement of phagocytic activity of both RAW264 cells and murine primary macrophages.

Five days of stimulation with rIL-18 or NFSA-CM increased the expression of *Nos2*, *IL-6* and *tnf-α,* which are well known as highly expressed genes in classical activated (that is M1-type) macrophages, in RAW264 cells (**Fig. 14**). It was previously reported that activated macrophages produced a variety of factors that were able to lyse tumor cells. These factors include TNF-α and nitric oxide (NO) (73, 74, 75, 76), which is mainly generated by inducible nitric synthase (*Nos2*). In addition, the expression of *Arg-1* was not detected and the expression of *IL-10* was decreased in RAW264 cells (**Fig. 14**). The addition of a neutralizing anti-IL-18 antibody reduced the expression of *Nos2*, *IL-6* and *tnf-α* in peritoneal macrophages. Thus, these results indicate that IL-18 in NFSA-CM is responsible for polarization of M1-type macrophages.

Heike et al. reported that the induction of *Nos2* in murine peritoneal macrophages upon treatment with IL-18 and IL-12 was mediated by IFN-γ (46). Bogdan et al. suggest that the induction of *Nos2* in macrophages requires the cooperation of other cells, such as lymphocytes or NK cells, which produce IFN-γ (77). Contrary to this, the expression of *Nos2* was induced only by stimulation with IL-18 for 5 days in this report. No detectable level of *IL-12p40*, a subunit of *IL12p70*, was detected in IL-18-stimulated RAW264 cells (**Fig. 15A**). In addition, the expression of *IL12p35,* the other subunit of *IL-12p70* (**Fig. 15A**), was not increased by the stimulation of IL-18 or NFSA-CM in RAW264 cells. Moreover, after the stimulation with rIL-18 or NFSA-CM, the expression of *IFN-γ* was not induced in RAW264 cells, contrarily, it was decreased significently (**Fig. 15B**). These data indicated that the IL-12 was not produced from RAW264 cells by IL-18-stiulation. Therefore, it indicated that IL-18 alone could program RAW264 cells to express *Nos2* in addition to other M1-macrophages markers.

Thus, we conclude that IL-18 alone contributes to program RAW264 cells to M1-like population, which showed some of the typical characters of M1-type macrophages, without disturbing the expression of its receptors after 5-days stimulation. This progress might be induced by via an *IFN-γ* independent pathway. The similar results were obtained in murine primary macrophages. Both IL-18 and NFSA-CM were responsible for increasing the expression of

M1-marker genes without disturbing the expression of M2-marker genes (**Fig. 16**). The addition of a neutralizing anti-IL-18 antibody reduced the expression of *Nos2*, *IL-6* and *tnf-α* and induced the expression of *IL-10* in peritoneal macrophages (**Fig. 16**). Neither IL-18 nor NFSA-CM was effective for inducing the expression of *IL-12p35* and *IL-12p40* (**Fig. 17**). These results indicate that IL-18 alone in NFSA-CM is responsible for polarization of M1-like macrophages in murine primary macrophages. However, when blocking the activity of IL-18 with neutralizing antibody, the expression of *IL-18r1* was down regulated (**Fig. 17**), suggesting that IL-18 might be important for supporting the expression of *IL-18r1* in murine primary macrophages.

Finally, the influence of the stimulated RAW264 cells on endothelial cells was analyzed using the F-2-Orange cells. The F-2-Orange cells were damaged more severely by the direct co-culture with the NFSA-CM- or IL-18-stimulated RAW cells (**Fig. 18, 19**). Thus, it suggests that some factors produced from NFSA cells, such as IL-18, enhance the cytotoxicity of macrophages to endothelial cells. Furthermore, the damage to the endothelium might be associated with soluble mediators produced from stimulated macrophages, such as pro-inflammatory factors and *Nos2*-derived NO.

NO is a critical biological mediator, which can take part in regulating blood vessel tone in vascular systems, and is an important host defence effector in the immune system. More importantly, the NO acts as a free oxygen radical and can act as a cytotoxic agent in pathological processes (65). Base on previous results, the IL-18- or NFSA-CM-stimulated RAW264 cells showed enhanced cytotoxicity to F-2-Orange cells, in addition to increasing expressed *Nos2*, the predominant generator of NO (65). In these cases, we challenged the effect of inhibiting the activity of NOS2 using 1400w. Since the inhibition of NOS2 by the inhibitor clearly inhibited the damaging of the endothelial cells, the NO was certainly one of the factors.

These results provide strong evidence that IL-18 stimulates the macrophages, and the phagocytosis and cytotoxicity to endothelium of them

are enhanced. Thus the angiogenesis in NFSA tumor is damaged. It may be the reason of necrosis in NFSA tumors (**Fig. 20**).

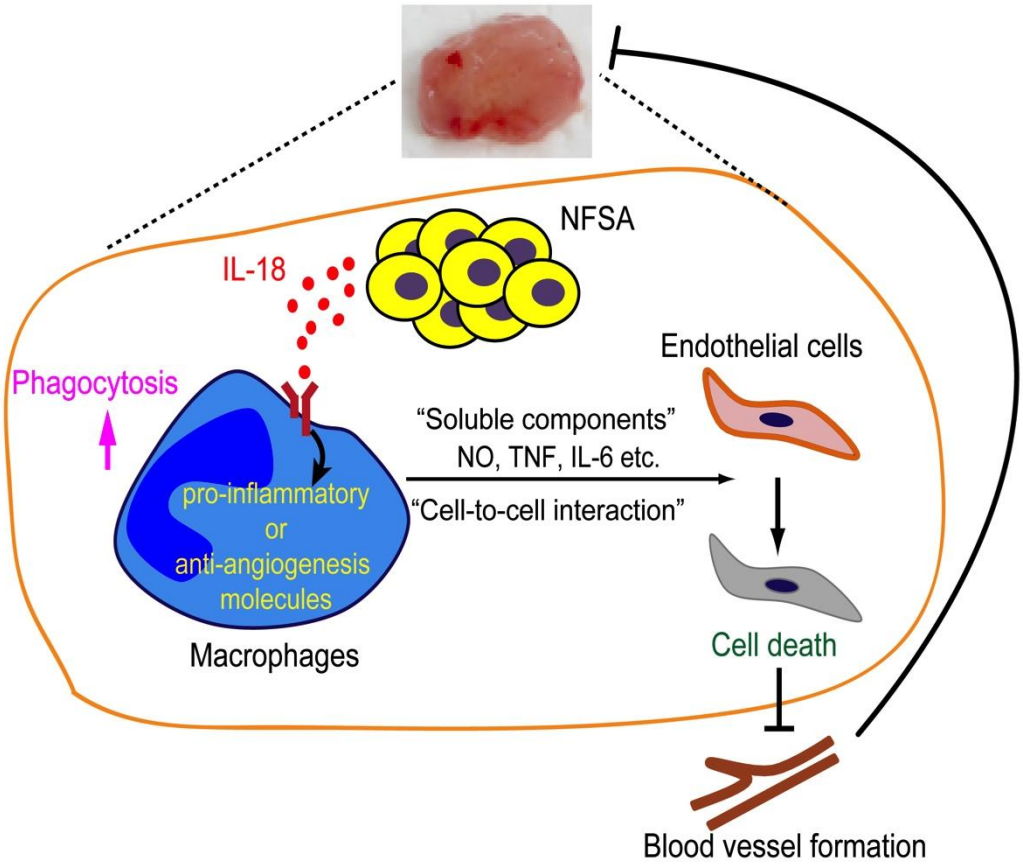

Figure 20. Hypothetical model of the anti-angiogenesis functions of macrophages in response to fibrosarcoma-produced IL-18.

IL-18 produced from a NFSA tumor enhances the phagocytic activity of macrophages and induces the expression of NO, TNF-α and IL-6. The activated macrophages damage endothelial cells and inhibit blood vessel formation in the NFSA tumor.

References

[1] Folkman, J. (1971) Tumor angiogenesis: therapeutic implications. N Engl J Med., pp 1182-1186

[2] Ding, Y. T., Kumar, S. and Yu, D. C. (2008) The Role of Endothelial Progenitor Cells in Tumour Vasculogenesis. Pathobiology. 75, 265-273.

[3] Murdoch, C., Muthana, M., Coffelt, S. B. and Lewis, C. E. (2008) The role of myeloid cells in the promotion of tumour angiogenesis. Nature Reviews Cancer. 8, 618-631.

[4] Biswas, S. K., Sica, A. and Lewis, C. E. (2008) Plasticity of macrophage function during tumor progression: regulation by distinct molecular mechanisms. J Immunol. 180, 2011-2017.

[5] Mantovani, A., Germano, G., Marchesi, F., Locatelli, M. and Biswas, S. K. (2011) Cancer-promoting tumor-associated macrophages: new vistas and open questions. Eur J Immunol. 41, 2522-2525.

[6] Gordon, S. and Taylor, P. R. (2005) Monocyte and macrophage heterogeneity. Nat Rev Immunol. 5, 953-964.

[7] Mantovani, A., Sozzani, S., Locati, M., Allavena, P. and Sica, A. (2002) Macrophage polarization: tumor-associated macrophages as a paradigm for polarized M2 mononuclear phagocytes. Trends Immunol. 23, 549-555.

[8] Sica, A., Larghi, P., Mancino, A., Rubino, L., Porta, C., Totaro, M. G., Rimoldi, M., Biswas, S. K., Allavena, P. and Mantovani, A. (2008) Macrophage polarization in tumour progression. Semin Cancer Biol. 18, 349-355.

[9] Sica, A., Schioppa, T., Mantovani, A. and Allavena, P. (2006) Tumour-associated macrophages are a distinct M2 polarised population promoting tumour progression: potential targets of anti-cancer therapy. Eur J Cancer. 42, 717-727.

[10] Lewis, C. E. and Pollard, J. W. (2006) Distinct role of macrophages in different tumor microenvironments. Cancer Res. 66, 605-612.

[11] Zhang, X., Tian, W., Cai, X., Wang, X., Dang, W., Tang, H., Cao, H., Wang, L. and Chen, T. (2013) Hydrazinocurcumin Encapsuled Nanoparticles "Re-Educate" Tumor-Associated Macrophages and Exhibit Anti-Tumor

Effects on Breast Cancer Following STAT3 Suppression. Plos One. 8, e65896.

[12] Biswas, S. K. and Mantovani, A. (2010) Macrophage plasticity and interaction with lymphocyte subsets: cancer as a paradigm. Nat Immunol. 11, 889-896.

[13] Wang, Y. C., He, F., Feng, F., Liu, X. W., Dong, G. Y., Qin, H. Y., Hu, X. B., Zheng, M. H., Liang, L., Feng, L., Liang, Y. M. and Han, H. (2010) Notch signaling determines the M1 versus M2 polarization of macrophages in antitumor immune responses. Cancer Res. 70, 4840-4849.

[14] O'Shea, J. J. and Murray, P. J. (2008) Cytokine signaling modules in inflammatory responses. Immunity. 28, 477-487.

[15] Mantovani, A. and Locati, M. (2013) Tumor-associated macrophages as a paradigm of macrophage plasticity, diversity, and polarization: lessons and open questions. Arterioscler Thromb Vasc Biol. 33, 1478-1483.

[16] Qian, B. Z. and Pollard, J. W. (2010) Macrophage diversity enhances tumor progression and metastasis. Cell. 141, 39-51.

[17] Porta, C., Rimoldi, M., Raes, G., Brys, L., Ghezzi, P., Di Liberto, D., Dieli, F., Ghisletti, S., Natoli, G., De Baetselier, P., Mantovani, A. and Sica, A. (2009) Tolerance and M2 (alternative) macrophage polarization are related processes orchestrated by p50 nuclear factor kappaB. Proc Natl Acad Sci U S A. 106, 14978-14983.

[18] Gordon, S. (2003) Alternative activation of macrophages. Nat Rev Immunol. 3, 23-35.

[19] Martinez, F. O., Helming, L. and Gordon, S. (2009) Alternative activation of macrophages: an immunologic functional perspective. Annu Rev Immunol. 27, 451-483.

[20] Sica, A. and Bronte, V. (2007) Altered macrophage differentiation and immune dysfunction in tumor development. J Clin Invest. 117, 1155-1166.

[21] Sica, A. (2010) Role of tumour-associated macrophages in cancer-related inflammation. Exp Oncol. 32, 153-158.

[22] Rolny, C., Mazzone, M., Tugues, S., Laoui, D., Johansson, I., Coulon, C., Squadrito, M. L., Segura, I., Li, X., Knevels, E., Costa, S., Vinckier, S., Dresselaer, T., Akerud, P., De Mol, M., Salomaki, H., Phillipson, M., Wyns, S., Larsson, E., Buysschaert, I., Botling, J., Himmelreich, U., Van Ginderachter, J. A., De Palma, M., Dewerchin, M., Claesson-Welsh, L. and Carmeliet, P. (2011) HRG inhibits tumor growth and metastasis by inducing macrophage polarization and vessel normalization through downregulation of PlGF. Cancer Cell. 19, 31-44.

[23] Solinas, G., Germano, G., Mantovani, A. and Allavena, P. (2009) Tumor-associated macrophages (TAM) as major players of the cancer-related inflammation. J Leukocyte Biol. 86, 1065-1073.

[24] Weigert, A., Sekar, D. and Brune, B. (2009) Tumor-associated macrophages as targets for tumor immunotherapy. Immunotherapy. 1, 83-95.

[25] Tang, X., Mo, C., Wang, Y., Wei, D. and Xiao, H. (2013) Anti-tumour strategies aiming to target tumour-associated macrophages. Immunology. 138, 93-104.

[26] Okamura, H., Tsutsui, H., Komatsu, T., Yutsudo, M., Hakura, A., Tanimoto, T., Torigoe, K., Okura, T., Nukada, Y., Hattori, K., Akita, K., Namba, M., Tanabe, F., Konishi, K., Fukuda, S. and Kurimoto, M. (1995) Cloning of a New Cytokine That Induces Ifn-Gamma Production by T-Cells. Nature. 378, 88-91.

[27] Micallef, M. J., Ohtsuki, T., Kohno, K., Tanabe, F., Ushio, S., Namba, M., Tanimoto, T., Torigoe, K., Fuji, M., Ikeda, M., Fukuda, S. and Kurimoto, M. (1996) Interferon-gamma-inducing factor enhances T helper 1 cytokine production by stimulated human T cells: Synergism with interleukin-12 for interferon-gamma production. Eur J Immunol. 26, 1647-1651.

[28] Stoll, S., Jonuleit, H., Schmitt, E., Muller, G., Yamauchi, H., Kurimoto, M., Knop, J. and Enk, A. H. (1998) Production of functional IL-18 by different subtypes of murine and human dendritic cells (DC):

DC-derived IL-18 enhances IL-12-dependent Th1 development. Eur J Immunol. 28, 3231-3239.

[29] Tsutsui, H., Nakanishi, K., Matsui, K., Higashino, K., Okamura, H., Miyazawa, Y. and Kaneda, K. (1996) IFN-gamma-inducing factor up-regulates fas ligand-mediated cytotoxic activity of murine natural killer cell clones. J Immunol. 157, 3967-3973.

[30] Gerdes, N., Sukhova, G. K., Libby, P., Reynolds, R. S., Young, J. L. and Schonbeck, U. (2002) Expression of interleukin (IL)-18 and functional IL-18 receptor on human vascular endothelial cells, smooth muscle cells, and macrophages: Implications for atherogenesis. J Exp Med. 195, 245-257.

[31] Ushio, S., Namba, M., Okura, T., Hattori, K., Nukada, Y., Akita, K., Tanabe, F., Konishi, K., Micallef, M., Fujii, M., Torigoe, K., Tanimoto, T., Fukuda, S., Ikeda, M., Okamura, H. and Kurimoto, M. (1996) Cloning of the cDNA for human IFN-gamma-lnducing factor, expression in Escherichia coli, and studies on the biologic activities of the protein. J Immunol. 156, 4274-4279.

[32] Gu Y, Kuida K, Tsutsui H and Ku G, H. K. (1997) Activation of interferon-gamma inducing factor mediated by interleukin-1beta converting enzyme. Science. 275(5297), 206-209.

[33] Ghayur, T., Banerjee, S., Hugunin, M., Butler, D., Herzog, L., Carter, A., Quintal, L., Sekut, L., Talanian, R., Paskind, M., Wong, W., Kamen, R., Tracey, D. and Allen, H. (1997) Caspase-1 processes IFN-gamma-inducing factor and regulates LPS-induced IFN-gamma production. Nature. 386, 619-623.

[34] Dinarello, C. A. (1999) IL-18: A TH1-inducing, proinflammatory cytokine and new member of the IL-1 family. J Allergy Clin Immunol. 103, 11-24.

[35] van de Veerdonk, F. L., Netea, M. G., Dinarello, C. A. and Joosten, L. A. (2011) Inflammasome activation and IL-1beta and IL-18 processing during infection. Trends Immunol. 32, 110-116.

[36] Tse, B. W. C., Russell, P. J., Lochner, M., Forster, I. and Power, C. A. (2011) IL-18 Inhibits Growth of Murine Orthotopic Prostate Carcinomas

via Both Adaptive and Innate Immune Mechanisms. Plos One. 6, e24241-24212.

[37] Zheng, J. N., Pei, D. S., Mao, L. J., Liu, X. Y., Sun, F. H., Zhang, B. F., Liu, Y. Q., Liu, J. J., Li, W. and Han, D. (2010) Oncolytic adenovirus expressing interleukin-18 induces significant antitumor effects against melanoma in mice through inhibition of angiogenesis. Cancer Gene Ther. 17, 28-36.

[38] Nagai, H., Hara, I., Horikawa, T., Oka, M., Kamidono, S. and Ichihashi, M. (2002) Gene transfer of secreted-type modified interleukin-18 gene to B16F10 melanoma cells suppresses in vivo tumor growth through inhibition of tumor vessel formation. J Invest Dermatol. 119, 541-548.

[39] Tanaka, F., Hashimoto, W., Robbins, P. D., Lotze, M. T. and Tahara, H. (2002) Therapeutic and specific antitumor immunity induced by co-administration of immature dendritic cells and adenoviral vector expressing biologically active IL-18. Gene Ther. 9, 1480-1486.

[40] Coughlin, C. M., Salhany, K. E., Wysocka, M., Aruga, E., Kurzawa, H., Chang, A. E., Hunter, C. A., Fox, J. C., Trinchieri, G. and Lee, W. M. F. (1998) Interleukin-12 and interleukin-18 synergistically induce murine tumor regression which involves inhibition of angiogenesis. J Clin Invest. 101, 1441-1452.

[41] Hikosaka, S., Hara, I., Miyake, H., Hara, S. and Kamidono, S. (2004) Antitumor effect of simultaneous transfer of interleukin-12 and interleukin-18 genes and its mechanism in a mouse bladder cancer model. Int J Urol. 11, 647-652.

[42] Stuyt, R. J., Netea, M. G., Geijtenbeek, T. B., Kullberg, B. J., Dinarello, C. A. and van der Meer, J. W. (2003) Selective regulation of intercellular adhesion molecule-1 expression by interleukin-18 and interleukin-12 on human monocytes. Immunology. 110, 329-334.

[43] Morel, J. C., Park, C. C., Woods, J. M. and Koch, A. E. (2001) A novel role for interleukin-18 in adhesion molecule induction through NF kappa B and phosphatidylinositol (PI) 3-kinase-dependent signal transduction pathways. J Biol Chem. 276, 37069-37075.

[44] Netea, M. G., Kullberg, B. J., Verschueren, I. and Van der Meer, J. W. M. (2000) Interleukin-18 induces production of proinflammatory cytokines in mice: no intermediate role for the cytokines of the tumor necrosis factor family and interleukin-1 beta. Eur J Immunol. 30, 3057-3060.

[45] Coma, G., Pena, R., Blanco, J., Rosell, A., Borras, F. E., Este, J. A., Clotet, B., Ruiz, L., Parkhouse, R. M. E. and Bofill, M. (2006) Treatment of monocytes with interleukin (IL)-12 plus IL-18 stimulates survival, differentiation and the production of CXC chemokine ligands (CXCL)8, CXCL9 and CXCL10. Clin Exp Immunol. 145, 535-544.

[46] Schindler, H., Lutz, M. B., Rollinghoff, M. and Bogdan, C. (2001) The production of IFN-gamma by IL-12/IL-18-activated macrophages requires STAT4 signaling and is inhibited by IL-4. J Immunol. 166, 3075-3082.

[47] Raschke, W. C., Baird, S., Ralph, P. and Nakoinz, I. (1978) Functional Macrophage Cell Lines Transformed by Abelson Leukemia-Virus. Cell. 15, 261-267.

[48] Ando, K., Hunter, N. and Peters, L. J. (1979) Immunologically Nonspecific Enhancement of Artificial Lung Metastases in Tumor-Bearing Mice. Cancer Immunol Immun. 6, 151-156.

[49] Shirata, K., Suzuki, T., Yanaihara, N., Sugimoto, K. and Mori, K. J. (1991) Establishment of a Sarcoma Cell-Line, Ms-K, Expressing Ki-Ras Protooncogene Product from Mouse Bone-Marrow Stromal Cells. Biomed Pharmacother. 45, 1-8.

[50] Toda, K. I., Tsujioka, K., Maruguchi, Y., Ishii, K., Miyachi, Y., Kuribayashi, K. and Imamura, S. (1990) Establishment and Characterization of a Tumorigenic Murine Vascular Endothelial-Cell Line (F2). Cancer Res. 50, 5526-5530.

[51] Kim, S. F., Huri, D. A. and Snyder, S. H. (2005) Inducible nitric oxide synthase binds, S-nitrosylates, and activates cyclooxygenase-2. Science. 310, 1966-1970.

[52] Pollard, J. W. (2009) Trophic macrophages in development and disease. Nat Rev Immunol. 9, 259-270.

[53] Mantovani, A., Allavena, P., Sica, A. and Balkwill, F. (2008) Cancer-related inflammation. Nature. 454, 436-444.

[54] Poon, I. K., Hulett, M. D. and Parish, C. R. (2010) Molecular mechanisms of late apoptotic/necrotic cell clearance. Cell Death Differ. 17, 381-397.

[55] Tohyama, Y. and Yamamura, H. (2006) Complement-mediated phagocytosis - The role of Syk. Iubmb Life. 58, 304-308.

[56] Suganuma, H., Fahey, J. W., Bryan, K. E., Healy, Z. R. and Talalay, P. (2011) Stimulation of phagocytosis by sulforaphane. Biochem Bioph Res Co. 405, 146-151.

[57] Peng, J., Tsang, J. Y., Li, D., Niu, N., Ho, D. H., Lau, K. F., Lui, V. C., Lamb, J. R., Chen, Y. and Tam, P. K. (2013) Inhibition of TGF-beta signaling in combination with TLR7 ligation re-programs a tumoricidal phenotype in tumor-associated macrophages. Cancer Lett. 331, 239-249.

[58] Fujisaka, S., Usui, I., Bukhari, A., Ikutani, M., Oya, T., Kanatani, Y., Tsuneyama, K., Nagai, Y., Takatsu, K., Urakaze, M., Kobayashi, M. and Tobe, K. (2009) Regulatory mechanisms for adipose tissue M1 and M2 macrophages in diet-induced obese mice. Diabetes. 58, 2574-2582.

[59] Mantovani, A., Sica, A., Sozzani, S., Allavena, P., Vecchi, A. and Locati, M. (2004) The chemokine system in diverse forms of macrophage activation and polarization. Trends Immunol. 25, 677-686.

[60] Takeda, Y., Costa, S., Delamarre, E., Roncal, C., de Oliveira, R. L., Squadrito, M. L., Finisguerra, V., Deschoemaeker, S., Bruyere, F., Wenes, M., Hamm, A., Serneels, J., Magat, J., Bhattacharyya, T., Anisimov, A., Jordan, B. F., Alitalo, K., Maxwell, P., Gallez, B., Zhuang, Z. W., Saito, Y., Simons, M., De Palma, M. and Mazzone, M. (2011) Macrophage skewing by Phd2 haplodeficiency prevents ischaemia by inducing arteriogenesis. Nature. 479, 122-U153.

[61] Spence, S., Fitzsimons, A., Boyd, C. R., Kessler, J., Fitzgerald, D., Elliott, J., Gabhann, J. N., Smith, S., Sica, A., Hams, E., Saunders, S. P., Jefferies, C. A., Fallon, P. G., McAuley, D. F., Kissenpfennig, A. and

Johnston, J. A. (2013) Suppressors of Cytokine Signaling 2 and 3 Diametrically Control Macrophage Polarization. Immunity. 38, 66-78.

[62] Wolf, S. F., Sieburth, D. and Sypek, J. (1994) Interleukin 12: a key modulator of immune function. Stem Cells. 12, 154-168.

[63] Folkman, J. (2007) Angiogenesis: an organizing principle for drug discovery? Nat Rev Drug Discov. 6, 273-286.

[64] Bergers, G. and Benjamin, L. E. (2003) Tumorigenesis and the angiogenic switch. Nat Rev Cancer. 3, 401-410.

[65] Moncada, S., Palmer, R. M. and Higgs, E. A. (1991) Nitric oxide: physiology, pathophysiology, and pharmacology. Pharmacol Rev. 43, 109-142.

[66] Sozzani, S., Rusnati, M., Riboldi, E., Mitola, S. and Presta, M. (2007) Dendritic cell-endothelial cell cross-talk in angiogenesis. Trends Immunol. 28, 385-392.

[67] Saccani, A., Schioppa, T., Porta, C., Biswas, S. K., Nebuloni, M., Vago, L., Bottazzi, B., Colombo, M. P., Mantovani, A. and Sica, A. (2006) p50 nuclear factor-kappaB overexpression in tumor-associated macrophages inhibits M1 inflammatory responses and antitumor resistance. Cancer Res. 66, 11432-11440.

[68] Rey-Giraud, F., Hafner, M. and Ries, C. H. (2012) In vitro generation of monocyte-derived macrophages under serum-free conditions improves their tumor promoting functions. Plos One. 7, e42656.

[69] Hao, N. B., Lu, M. H., Fan, Y. H., Cao, Y. L., Zhang, Z. R. and Yang, S. M. (2012) Macrophages in Tumor Microenvironments and the Progression of Tumors. Clin Dev Immunol. 2012, 948098-948108.

[70] Mantovani, A. and Sica, A. (2010) Macrophages, innate immunity and cancer: balance, tolerance, and diversity. Curr Opin Immunol. 22, 231-237.

[71] Dunkelberger, J. R. and Song, W. C. (2010) Complement and its role in innate and adaptive immune responses. Cell Res. 20, 34-50.

[72] Daha, M. R. (2010) Role of Complement in Innate Immunity and Infections. Crit Rev Immunol. 30, 47-52.

[73] Hibbs, J. B., Taintor, R. R. and Vavrin, Z. (1987) Macrophage Cytotoxicity - Role for L-Arginine Deiminase and Imino-Nitrogen Oxidation to Nitrite. Science. 235, 473-476.

[74] Keller, R., Keist, R., Wechsler, A., Leist, T. P. and Vandermeide, P. H. (1990) Mechanisms of Macrophage-Mediated Tumor-Cell Killing - a Comparative-Analysis of the Roles of Reactive Nitrogen Intermediates and Tumor-Necrosis-Factor. Int J Cancer. 46, 682-686.

[75] Yamanishi, T., Hatakeyama, T., Yamaguchi, K. and Oda, T. (2009) CEL-I, an N-Acetylgalactosamine (GalNAc)-Specific C-Type Lectin, Induces Nitric Oxide Production in RAW264.7 Mouse Macrophage Cell Line. J Biochem. 146, 209-217.

[76] Engin, A. B. (2011) Dual Function of Nitric Oxide in Carcinogenesis, Reappraisal. Curr Drug Metab. 12, 891-899.

[77] Bogdan, C. and Schleicher, U. (2006) Production of interferon-gamma by myeloid cells - fact or fancy? Trends Immunol. 27, 282-290.

Acknowledgement

It has been a great privilege to spend several years in Sugimoto laboratory in Niigata University, and its members will always remain dear to me.

My first debt of gratitude must go to my supervisor, Dr. Sugimoto, a respectable, responsible and resourceful scholar. He patiently provided the vision, encouragement and advice necessary for me to precede through the doctorial program and complete my dissertation. His unflagging encouragement and serving as a role model to me as a junior member of academia.

Special thanks to Dr. Touma for her support, guidance and helpful suggestions. Her guidance has served me well and I owe her my heartfelt appreciation.

Members in Sugimoto Lab. also deserve my sincerest thanks, their friendship and assistance has meant more to me than I could ever express.

I should also show my appreciation to Dr. Maeno, Dr Uchiumi and all the faculty in Graduate School of Science and Technology who have helped me to develop the fundamental and essential academic competence.

Finally, I wish to thank my parents and grandma. Their love provided my inspiration and was my driving force. I owe them everything and wish I could show them just how much I love and appreciate them.